Inorg. Chem. **1997,** *36,* 1149−1163

Comparative Analysis of the Conformations of Symmetrically and Asymmetrically Deca- and Undecasubstituted Porphyrins Bearing Meso-Alkyl or -Aryl Groups

Mathias O. Senge,*[1a,b] Craig J. Medforth,[1a] Timothy P. Forsyth,[1a] David A. Lee,[1a] Marilyn M. Olmstead,[1a] Walter Jentzen,[1c] Ravindra K. Pandey,[1a] John A. Shelnutt,[1c] and Kevin M. Smith*[1a]

Department of Chemistry, University of California, Davis, California 95616, Institut für Organische Chemie (WE02), Freie Universität Berlin, Takustrasse 3, D-14195 Berlin, Germany, and Fuel Science Department, Sandia National Laboratories, Albuquerque, New Mexico 87185-0710

Received September 18, 1996[⊗]

Conformational analysis of highly substituted porphyrins has potential implications for modeling the behavior of macrocycles in tetrapyrrole-containing protein complexes and during catalytic reactions. In order to study the influence of different substituent patterns on the conformation of the porphyrin macrocycle, a series of metal free and nickel(II) decasubstituted porphyrins bearing aryl or ethyl groups at opposite meso positions and alkyl groups at the pyrrole positions have been synthesized and characterized by X-ray crystallography. Crystal structures of the free-base porphyrins with 5,15-diaryl substituents showed negligible out-of-plane distortion but a large amount of in-plane distortion along the 5,15-axis accompanied by large bond angle changes similar to those previously seen for related porphyrins with 5,15-dialkyl substituents. Nickel(II) complexes of the 5,15-diaryl-substituted porphyrins show planar or modestly nonplanar conformations, suggesting that these complexes are not intrinsically nonplanar, whereas a complex with 5,15-diethyl substituents has a very ruffled conformation similar to those observed for related complexes with other metals. The nickel(II) complexes are also elongated along the 5,15-axis in a qualitatively similar but less dramatic fashion than are the free-base porphyrins. Spectrosopic studies (^{1}H NMR, optical, and resonance Raman spectroscopy) suggest that conformations similar to those determined by X-ray crystallography are present in solution for the 5,15-dialkyl- and 5,15-diaryl-substituted porphyrins. Several asymmetric nickel(II) and metal-free deca- and undecasubstituted porphyrins containing both aryl and alkyl meso-substituents were also investigated. Metal-free 5,15-disubstituted porphyrins with one aryl and one alkyl group showed considerably elongated porphyrin cores, whereas nickel(II) complexes of porphyrins with 5,10- or 5,10,15-substitution patterns showed very nonplanar structures consisting mainly of ruffle and saddle type distortions.

Introduction

The conformations of porphyrins are currently under active scrutiny with regard to the connection between macrocycle distortion and physicochemical properties.[2,3] The flexibility of the tetrapyrrole system was demonstrated in the early porphyrin crystal structures of Hoard,[4] and since then, a considerable body of information has been accumulated about how the conformations of simple porphyrin compounds such as octaethylporphyrin (OEP, **1**) and tetraphenylporphyrin (TPP, **2**) can be influenced by metal, packing, and axial ligand effects.[5] The concept of conformationally flexible tetrapyrrole macrocycles has wide implications for the study of chromophore−protein interactions *in vivo*.[2,3,6] Some years ago, it was realized that the conformational flexibility might modulate the biological properties of tetrapyrroles *in vivo*,[2] and nonplanar tetrapyrrole conformations have been observed in the bacterial photosynthetic reaction center,[7] a photosynthetic antenna complex,[8] heme proteins,[9] methyl reductase,[10] and vitamin B$_{12}$-dependent enzymes.[11]

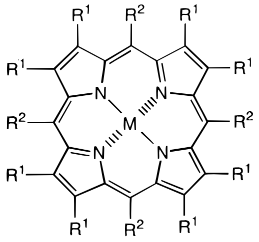

	R^1	**R^2**
1	CH$_2$CH$_3$	H
2	H	C$_6$H$_5$
3	CH$_2$CH$_3$	C$_6$H$_5$
4	C$_6$H$_5$	C$_6$H$_5$
5a	-(CH$_2$)$_3$-	CH$_3$
5b	-(CH$_2$)$_3$-	CH$_2$CH$_3$
5c	-(CH$_2$)$_3$-	(CH$_2$)$_4$CH$_3$
6	Br or Cl	C$_6$H$_5$
7	CH$_2$CH$_3$	NO$_2$
8	H	C(CH$_3$)$_3$

Physical studies have shown a direct correlation between macrocycle nonplanarity and properties such as spin delocalization, redox potential, and the positions of optical absorption

---

[⊗] Abstract published in *Advance ACS Abstracts,* February 15, 1997.

(1) (a) University of California. (b) Permanent address: Freie Universität Berlin. (c) Sandia National Laboratories.

(2) Barkigia, K. M.; Chantranupong, L.; Smith, K. M.; Fajer, J. *J. Am. Chem. Soc.* **1988**, *110*, 7566.

(3) (a) Fajer, J. *Chem. Ind.* **1991**, 869. (b) Senge, M. O. *J. Photochem. Photobiol., B* **1992**, *16*, 3. (c) Ravikanth, M.; Chandrashekar, T. K. *Struct. Bonding (Berlin)* **1995**, *82*, 105.

(4) Hoard, J. L. *Science* **1971**, *174*, 1295; *Ann. N.Y. Acad. Sci.* **1973**, *206*, 18.

(5) Scheidt, W. R.; Lee, Y. J. *Struct. Bonding (Berlin)* **1987**, *64*, 1.

(6) (a) Eschenmoser, A. *Ann. N.Y. Acad. Sci.* **1986**, *471*, 108. (b) Horning, T. L.; Fujita, E.; Fajer, J. *J. Am. Chem. Soc.* **1986**, *108*, 323. Fajer, J.; Barkigia, K. M.; Smith, K. M.; Zhong, E.; Gudowska-Nowak, E.; Newton, M. In *Reaction Centers of Photosynthetic Bacteria*; Michel-Beyerle, M. E., Ed.; Springer Verlag: Berlin, 1990; p 367. (c) Huber, R. *Eur. J. Biochem.* **1990**, *187*, 283.

(7) Deisenhofer, J.; Michel, H. *Angew. Chem., Int. Ed. Engl.* **1989**, *28*, 829. Deisenhofer, J.; Epp, O.; Miki, K.; Huber, R.; Michel, H. *J. Mol. Biol.* **1984**, *180*, 385. Michel, H.; Epp, O.; Deisenhofer, J. *EMBO J.* **1986**, *5*, 2445. Yeates, T. O.; Komiya, H.; Chirino, A.; Rees, D. C.; Allen, J. P.; Feher, G. *Proc. Natl. Acad. Sci. U.S.A.* **1988**, *85*, 7993.

(8) Fenna, R. E.; Matthews, B. W. *Nature* **1975**, *258*, 573. Tronrud, D. E.; Schmid, M. F.; Matthews, B. W. *J. Mol. Biol.* **1986**, *188*, 443.

S0020-1669(96)01156-1 CCC: $14.00

and resonance Raman bands.[3c] Theoretical studies on the bacteriochlorophylls have also indicated that the observed individual absorption bands in pigment protein complexes can be correlated to the conformation of the individual chlorophylls.[2,12a] The unidirectionality of the electron transfer in the bacterial photosynthetic reaction center has also been attributed to specific "structural engineering" of the prosthetic groups,[12b] and ruffling of the porphyrin core has been proposed to play a role in the ligand binding function of heme.[12c] Recently, specific heme distortions were found to be conserved for mitochondrial and some other cytochromes *c* from diverse species, further implying a biological role for such ring distortions.[13] Model compounds employed in contemporary studies are mainly dodecasubstituted porphyrins with S_4 symmetry.[14−21] Examples include 2,3,7,8,12,13,17,18-octaethyl-5,10,15,20-tetraphenylporphyrin (OETPP, **3**),[2,14,15] dodecaphenylporphyrin (DPP, **4**),[16,17] TPP with alkano rings enclosing the C_b-C_b positions (**5**),[18] 2,3,7,8,12,13,17-octahalogeno-TPP derivatives (**6**),[19] and 5,10,15,20-tetranitro-OEP (**7**).[20] In most cases, highly nonplanar saddle[22] conformations were observed due to steric interaction of the meso-substituents with neighboring C_b substituents. Quite different ruffle[22] conformations were observed in 5,10,15,20-tetrasubstituted porphyrins with very bulky groups, e.g. 5,10,15,20-tetra-*tert*-butylporphyrin (TtBuP, **8**).[21]

Although the possibility of steric strain in mono- and di-meso-substituted OEP derivatives was pointed out by Woodward[23] during his elegant synthetic studies of chlorophyll, less symmetric porphyrins have not attracted much interest within the context of recent conformational analyses. However, historically the first crystallographic proof of porphyrin nonplanarity induced by peripheral substituents was found for a mono-meso-substituted OEP derivative. Such compounds were therefore labeled "highly substituted porphyrins".[24] Crystallographic and spectroscopic evidence has since been obtained for nonplanar conformational distortions in a number of mono- and di-meso-substituted porphyrins, although the compounds studied are too unrelated to allow the identification of general trends.[24−35] A

---

(9) (a) Huber, R.; Epp, O.; Formanek, H. *J. Mol. Biol.* **1970**, *52*, 349. Anderson, L. *J. Mol. Biol.* **1973**, *79*, 495. Heidner, E.; Ladner, R. C.; Perutz, M. F. *J. Mol. Biol.* **1976**, *104*, 707. Deatherage, J. F.; Loe, R. S.; Anderson, C. M.; Moffat, K. *J. Mol. Biol.* **1976**, *104*, 687. Moffat, K.; Loe, R. S.; Hoffman, B. M. *J. Mol. Biol.* **1976**, *104*, 669. Takano, T. *J. Mol. Biol.* **1977**, *110*, 537. Ladner, R. C.; Heidner, E. J.; Perutz, M. F. *J. Mol. Biol.* **1977**, *114*, 385. (b) Alden, R. G.; Ondrias, M. R.; Shelnutt, J. A. *J. Am. Chem. Soc.* **1990**, *112*, 691. (c) Crane, B. R.; Siegel, L. M.; Getzoff, E. D. *Science* **1995**, *270*, 60.

(10) Zimmer, M.; Crabtree, R. H. *J. Am. Chem. Soc.* **1990**, *112*, 1062. Furenlid, D. E.; Renner, M. W.; Smith, K. M.; Fajer, J. *J. Am. Chem. Soc.* **1990**, *112*, 1634. Furenlid, D. E.; Renner, M. W.; Fajer, J. *J. Am. Chem. Soc.* **1990**, *112*, 8987.

(11) Geno, M. K.; Halpern, J. *J. Am. Chem. Soc.* **1987**, *109*, 1238. Drennan, C. L.; Huang, S.; Drummond, J. T.; Matthews, R. G.; Ludwig, M. L. *Science* **1994**, *266*, 1669. Kräutler, B.; Konrat, R.; Stupperich, E.; Färber, G.; Gruber, K.; Kratky, C. *Inorg. Chem.* **1994**, *33*, 4128. Kratky, C.; Färber, G.; Gruber, K.; Wilson, K.; Dauter, Z.; Nolting, H.-F.; Konrat, R.; Kräutler, B. *J. Am. Chem. Soc.* **1995**, *117*, 4654.

(12) (a) Gudowska-Nowak, E.; Newton, M. D.; Fajer, J. *J. Phys. Chem.* **1990**, *94*, 5795. Thompson, M. A.; Zerner, M. C.; Fajer, J. *J. Phys. Chem.* **1991**, *95*, 5693. (b) Plato, M.; Möbius, K.; Michel-Beyerle, M. E.; Bixon, M.; Jortner, J. *J. Am. Chem. Soc.* **1988**, *110*, 7279. (c) Baltzer, L.; Landergren, M. *J. Am. Chem. Soc.* **1990**, *112*, 2804.

(13) Hobbs, J. D.; Shelnutt, J. A. *J. Protein Chem.* **1995**, *14*, 19.

(14) Dolphin, D. *J. Heterocycl. Chem.* **1970**, *7*, 275. Evans, B.; Smith, K. M.; Fuhrhop, J.-H. *Tetrahedron Lett.* **1977**, *5*, 443.

(15) (a) Barkigia, K. M.; Berber, M. D.; Fajer, J.; Medforth, C. J.; Renner, M. W.; Smith, K. M. *J. Am. Chem. Soc.* **1990**, *112*, 8851. (b) Sparks, L. D.; Medforth, C. J.; Park, M.-S.; Chamberlain, J. R.; Ondrias, M. R.; Senge, M. O.; Smith, K. M.; Shelnutt, J. A. *J. Am. Chem. Soc.* **1993**, *115*, 581. (c) Barkigia, K. M.; Renner, M. W.; Furenlid, L. R.; Medforth, C. J.; Smith, K. M.; Fajer, J. *J. Am. Chem. Soc.* **1993**, *115*, 3627. (d) Stichternath, A.; Schweitzer-Stenner, R.; Dreybrodt, W.; Mak, R. S. W.; Li, X.-Y.; Sparks, L. D.; Shelnutt, J. A.; Medforth, C. J.; Smith, K. M. *J. Phys. Chem.* **1993**, *97*, 3701. (e) Gentemann, S.; Medforth, C. J.; Forsyth, T. P.; Nurco, D. J.; Smith, K. M.; Fajer, J.; Holten, D. *J. Am. Chem. Soc.* **1994**, *116*, 7363. (f) Renner, M. W.; Barkigia, K. M.; Zhang, Y.; Medforth, C. J.; Smith, K. M.; Fajer, J. *J. Am. Chem. Soc.* **1994**, *116*, 8582. (g) Regev, A.; Galili, T.; Medforth, C. J.; Smith, K. M.; Barkigia, K. M.; Fajer, J.; Levanon, H. *J. Phys. Chem.* **1994**, *98*, 2520. (h) Senge, M. O.; Forsyth, T. P.; Nguyen, L. T.; Smith, K. M. *Angew. Chem., Int. Ed. Engl.* **1994**, *33*, 2485. (i) Kadish, K. M.; Van Caemelbecke, E.; D'Souza, F.; Medforth, C. J.; Smith, K. M.; Tabard, A.; Guilard, R. *Inorg. Chem.* **1995**, *34*, 2984.

(16) (a) Medforth, C. J.; Smith, K. M. *Tetrahedron Lett.* **1990**, *31*, 5583. (b) Medforth, C. J.; Senge, M. O.; Smith, K. M.; Sparks, L. D.; Shelnutt, J. A. *J. Am. Chem. Soc.* **1992**, *114*, 9859.

(17) Tsuchiya, S. *Chem. Phys. Lett.* **1990**, *169*, 608; *J. Chem. Soc., Chem. Commun.* **1991**, 716; **1992**, 1745. Takeda, J.; Ohya, T.; Sato, M. *Chem. Phys. Lett.* **1991**, *183*, 384; *Inorg. Chem.* **1992**, *31*, 2877. Takeda, J.; Sato, M. *Chem. Lett.* **1995**, 939, 971.

(18) (a) Medforth, C. J.; Berber, M. D.; Smith, K. M.; Shelnutt, J. A. *Tetrahedron Lett.* **1990**, *31*, 3719. (b) Shelnutt, J. A.; Medforth, C. J.; Berber, M. D.; Barkigia, K. M.; Smith, K. M. *J. Am. Chem. Soc.* **1991**, *113*, 4077. (c) Senge, M. O.; Medforth, C. J.; Sparks, L. D.; Shelnutt, J. A.; Smith, K. M. *Inorg. Chem.* **1993**, *32*, 1716. (d) Choi, S.; Phillips, J. A.; Ware, W., Jr.; Wittschieben, C.; Medforth, C. J.; Smith, K. M. *Inorg. Chem.* **1994**, *33*, 3873.

(19) (a) Bhyrappa, P.; Krishnan, V. *Inorg. Chem.* **1991**, *30*, 239. (b) Mandon, D.; Ochsenbein, P.; Fischer, J.; Weiss, R.; Jayaraj, K.; Austin, R. N.; Gold, A.; White, P. S.; Brigaud, O.; Battioni, P.; Mansuy, D. *Inorg. Chem.* **1992**, *31*, 2044. Schaefer, W. P.; Hodge, J. A.; Hughes, M. E.; Gray, H. B.; Lyons, J. E.; Ellis, P. E., Jr.; Wagner, R. W. *Acta Crystallogr.* **1993**, *C49*, 1342. Henling, L. M.; Schaefer, W. P.; Hodge, J. A.; Hughes, M. E.; Gray, H. B. *Acta Crystallogr.* **1993**, *C49*, 1743. Marsh, R. E.; Schaefer, W. P.; Hodge, J. A.; Hughes, M. E.; Gray, H. B. *Acta Crystallogr.* **1993**, *C49*, 1339. Takeuchi, T.; Gray, H. B.; Goddard, W. A., III. *J. Am. Chem. Soc.* **1994**, *116*, 9730. Hodge, J. A.; Hill, M. G.; Gray, H. B. *Inorg. Chem.* **1995**, *34*, 809. Birnbaum, E. R.; Hodge, J. A.; Grinstaff, M. W.; Schaefer, W. P.; Henling, L.; Labinger, J. A.; Bercaw, J. E.; Gray, H. B. *Inorg. Chem.* **1995**, *34*, 3625. Birnbaum, E. R.; Schaefer, W. P.; Labinger, J. A.; Bercaw, J. E.; Gray, H. B. *Inorg. Chem.* **1995**, *34*, 1751. (c) Bhyrappa, P.; Krishnan, V.; Nethaji, M. *J. Chem. Soc., Dalton Trans.* **1993**, 1901; *Chem. Lett.* **1993**, 869. Ochsenbein, P.; Mandon, D.; Fischer, J.; Weiss, R.; Austin, R. N.; Jayaraj, K.; Gold, A.; Terner, J.; Bill, E.; Müther, M.; Trautwein, A. X. *Angew. Chem., Int. Ed. Engl.* **1993**, *32*, 1437. Ochsenbein, P.; Akoyougou, K.; Mandon, D.; Fischer, J.; Weiss, R.; Austin, R. N.; Jayaraj, K.; Gold, A.; Terner, J.; Fajer, J. *Angew. Chem., Int. Ed. Engl.* **1994**, *33*, 348.

(20) (a) Gong, L.-C.; Dolphin, D. *Can. J. Chem.* **1985**, *63*, 401. (b) Zhu, N.-J.; Li, Y.; Wu, G.-Z.; Liang, X.-G. *Acta Chim. Sin.* **1992**, *50*, 249. (c) Senge, M. O. *J. Chem. Soc., Dalton Trans.* **1993**, 3539. (d) Senge, M. O.; Smith, K. M. *J. Chem. Soc., Chem. Commun.* **1994**, 923. (e) Hobbs, J. D.; Majumder, S. A.; Luo, L.; Sickelsmith, G. A.; Quirke, J. M. E.; Medforth, C. J.; Smith, K. M.; Shelnutt, J. A. *J. Am. Chem. Soc.* **1994**, *116*, 3261.

(21) (a) Ema, T.; Senge, M. O.; Nelson, N. Y.; Ogoshi, H.; Smith, K. M. *Angew. Chem., Int. Ed. Engl.* **1994**, *33*, 1879. (b) Senge, M. O.; Ema, T.; Smith, K. M. *J. Chem. Soc., Chem. Commun.* **1995**, 733.

(22) The terms "ruffled" and "saddle conformations" are used as defined by Scheidt and Lee.[5] A saddle conformation is characterized by alternate pyrrole ring displacements above and below a least-squares plane through the 24 core atoms. A ruffled conformation has alternate pyrrole rings that are alternately twisted clockwise and counterclockwise about the M−N bond such that the meso-carbons are alternately above and below the least-squares plane of the macrocycle core atoms.

(23) Woodward, R. B. *Angew. Chem.* **1960**, *72*, 651.

(24) (a) Hursthouse, M. B.; Neidle, S. *J. Chem. Soc., Chem. Commun.* **1972**, 449. Neidle, S.; Hursthouse, M. B. *Acta Crystallogr.* **1978**, *34*, 2509. (b) Fuhrhop, J.-H.; Witte, L.; Sheldrick, W. S. *Liebigs Ann. Chem.* **1976**, 1537.

(25) (a) Buchler, J. W.; Puppe, L. *Liebigs Ann. Chem.* **1970**, *740*, 142. (b) Lay, K.-L.; Buchler, J. W.; Kenny, J. E.; Scheidt, W. R. *Inorg. Chim. Acta* **1986**, *123*, 91.

(26) Abraham, R. J.; Jackson, A. H.; Kenner, G. W.; Warburton, D. *J. Chem. Soc.* **1963**, 853. Smith, K. M.; Bobe, F. W.; Minnetian, O. M. *Tetrahedron* **1984**, *40*, 3263.

(27) (a) Sheldrick, W. S. *Acta Crystallogr.* **1977**, *B33*, 3967; (b) *Acta Crystallogr.* **1978**, *B34*, 663.

(28) (a) Hitchcock, P. B. *J. Chem. Soc., Dalton Trans.* **1983**, 6747. (b) Collman, J. P.; Chong, A. O.; Jameson, G. B.; Oakley, R. T.; Rose, E.; Schmittou, E. R.; Ibers, J. A. *J. Am. Chem. Soc.* **1981**, *103*, 516. (c) Fillers, J. P.; Ravichandran, K. G.; Abdalmuhdi, I.; Tulinsky, A.; Chang C. K. *J. Am. Chem. Soc.* **1986**, *108*, 417.

(29) Maruyama, K.; Nagata, T.; Osuka, A. *J. Phys. Org. Chem.* **1988**, *1*, 63.

number of reports on the synthesis of 5,15-disubstituted porphyrins have also appeared,[29,33,36] but no detailed analysis of their conformations has heretofore been performed.

As a first step to understanding the conformational properties of 5,15-disubstituted porphyrins, we recently reported a study of the free base, nickel(II), and zinc(II) complexes of the decaalkylporphyrin **9**.[35] An interesting feature of the crystal structure of metal-free **9** (**H₂9**) was an essentially planar conformation of the macrocycle, with steric strain between the meso and pyrrole ethyl substituents being relieved by a novel elongation of the macrocycle along the 5,15-axis. To see if such elongation is a general feature of this class of porphyrins and to understand the influence of different 5,15-substituents (e.g., aryl vs ethyl) on the porphyrin conformation, we have synthesized the nickel(II) and metal-free forms of compounds **10−13** and determined the structures of these porphyrins using X-ray crystallography. The solution conformations of the porphyrins were also probed with a range of techniques including proton NMR, optical, and resonance Raman spectroscopy. In addition, X-ray crystal structures were obtained for a limited number of asymmetrically decasubstituted porphyrins (**14−16**) and undecasubstituted porphyrins (**17**, **18**) to investigate the effect of different substitution patterns on the degree and type of nonplanar distortion.

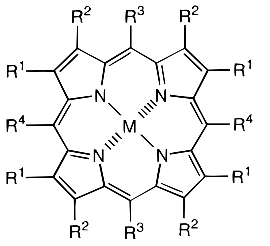

	R¹	R²	R³	R⁴
9	CH_2CH_3	CH_3	H	CH_2CH_3
10	CH_3	CH_2CH_3	H	CH_2CH_3
11	CH_3	CH_2CH_3	H	C_6H_5
12	CH_3	CH_2CH_3	H	C_6H_3-2,5-OCH_3
13	CH_3	$(CH_2)_3CH_3$	H	C_6H_4N

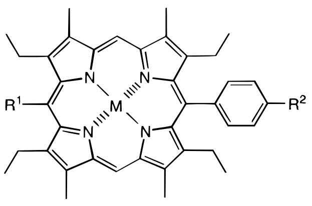

14 R^1 = OH, R^2 = H
15 R^1 = Cl, R^2 = CH_2Cl

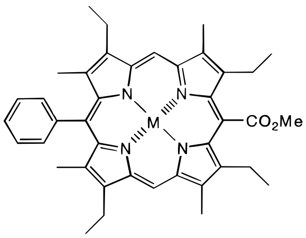

16

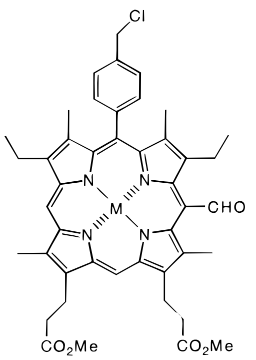

17

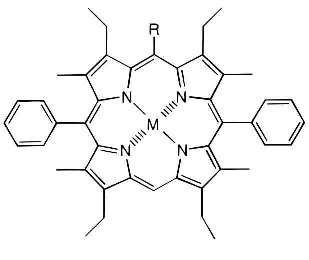

18 R = $CH{=}CHCO_2CH_2CH_3$
19 R = CHO

Experimental Section

General Procedures. Chemicals and solvents used were of analytical grade and were purchased commerically. Melting points are uncorrected and were measured on a Bristoline hot stage apparatus. Silica gel 60 (70−230 and 230−400 mesh, Merck) or neutral alumina (Merck, usually Brockmann Grade III, i.e. deactivated with 6% water) was used for column chromatography. Analytical thin-layer chromatography (TLC) was carried out using Merck 60 F254 silica gel (precoated sheets, 0.2 mm thick). Reactions were monitored by TLC and spectrophotometry and were carried out in dimmed light.

Proton NMR spectra were recorded at a frequency of 300 MHz. The chemical shifts are given in ppm and have been converted to the δ scale using the solvent signal at 5.30 δ for CD_2Cl_2 or 7.26 δ for $CDCl_3$. The variable-temperature unit was calibrated using a sample of methanol.[37] Electronic absorption spectra were recorded on a Hewlett Packard 8450A spectrophotometer using dichloromethane as solvent. Mass spectra were obtained at the Mass Spectrometry Facility, University of California, San Francisco, on a VG Analytical ZAB-HS-2F mass spectrometer, using a direct-insertion probe. High-resolution spectra were acquired at 70 eV, 50 mA, and a source temperature of 200 °C. Raman difference spectra were obtained using procedures described elsewhere.[15b,18b]

Syntheses. The syntheses of metal-free compounds **H₂11**,[38a] **H₂12**,[33b] **H₂14**,[38b] and **H₂15**[38b] **H₂16**,[38b] and nickel complexes **Ni17**,[38a] **Ni18**,[38a] and **Ni19**[38a] are described elsewhere. Metal complexes were prepared from the corresponding free-base porphyrins using standard methodology.[39]

(a) H₂10. Step 1. 1,1-Bis(5-(ethoxycarbonyl)-4-ethyl-3-methylpyrrol-2-yl)propane. A solution of 2-(ethoxycarbonyl)-3-ethyl-4-methylpyrrole[40a] (10.4 g, 57.4 mmol) in 200 mL of benzene was heated to reflux under nitrogen. A catalytic quantity (0.5 g) of *p*-TsOH was added, followed by propionaldehyde (6.6 g, 114 mmol). The mixture was refluxed overnight using a Dean Stark trap to remove water, after which it was cooled to room temperature, washed with sodium bicarbonate (3 × 100 mL) and water (1 × 100 mL), and dried over anhydrous sodium sulfate. The light brown solution was concentrated in vacuo to yield a brown waxy solid. The solid was triturated with hot pentane and filtered off. Yield: 8.8 g (74%) as a white flocculent powder. Mp: 151 °C. ^{1}H-NMR ($CDCl_3$): δ 9.35 (br s, 1H, NH),

---

(30) Nagata, T.; Osuka, A.; Maruyama, K.; Toriumi, K. *Acta Crystallogr.* **1990**, *C46*, 1745.

(31) (a) Senge, M. O.; Liddell, P. A.; Smith, K. M. *Acta Crystallogr.* **1992**, *C48*, 581. (b) Senge, M. O.; Forsyth, T. P.; Smith, K. M. *Z. Kristallogr.* **1996**, *211*, 176.

(32) Senge, M. O.; Vicente, M. G. H.; Parkin, S. R.; Hope, H.; Smith, K. M. *Z. Naturforsch.* **1992**, *47B*, 1189.

(33) (a) Hombrecher, H. K.; Horter, G. *Liebigs Ann. Chem.* **1991**, 219. (b) Hombrecher, H. K.; Horter, G.; Arp, C. *Tetrahedron* **1992**, *48*, 9451.

(34) (a) Anderson, H. L.; Hunter, C. A.; Sanders, J. K. M. *J. Chem. Soc., Chem. Commun.* **1989**, 226. (b) Roeterdink, F.; van der Plas, H. C. *J. Heterocycl. Chem.* **1990**, *27*, 1733.

(35) Medforth, C. J.; Senge, M. O.; Forsyth, T. P.; Hobbs, J. D.; Shelnutt, J. A.; Smith, K. M. *Inorg. Chem.* **1994**, *33*, 3865.

(36) Baldwin, J. E.; Klose, T.; Peters, M. *J. Chem. Soc., Chem. Commun.* **1976**, 88. Ogoshi, H.; Sugimoto, H.; Nishiguchi, T.; Watanabe, T.; Matsuda, Y.; Yoshida, Z. *Chem. Lett.* **1978**, 29. Gunter, M. J.; Mander, L. N. *J. Org. Chem.* **1981**, *46*, 4792. Gunter, M. J.; Mander, L. N.; Murry, K. S.; Clark, P. E. *J. Am. Chem. Soc.* **1981**, *103*, 6784. Young, R.; Chang, C. K. *J. Am. Chem. Soc.* **1985**, *107*, 898. Aoyama, Y.; Uzawa, T.; Saita, K.; Tanaka, Y.; Toi, H.; Ogoshi, H.; Okamoto, Y. *Tetrahedron Lett.* **1988**, *29*, 5271. Sanders, G. M.; van Dijk, M.; van Veldhuizen, A.; van der Plas, H. C.; Hostra, U.; Schaafsma, T. J. *J. Org. Chem.* **1988**, *53*, 5272. Osuka, A.; Yamada, H.; Maruyama, K. *Chem. Lett.* **1990**, 1905. Osuka, A.; Nagata, T.; Kobayashi, F.; Maruyama, K. *J. Heterocycl. Chem.* **1990**, *27*, 1657.

(37) van Geet, A. L. *Anal. Chem.* **1970**, *42*, 679.

(38) (a) Pandey, R. K.; Smith, K. M. Manuscript in preparation. (b) Lee, D. A.; Smith, K. M. Manuscript in preparation.

(39) Smith, K. M., Ed. *Porphyrins and Metalloporphyrins*; Elsevier: Amsterdam, 1975.

(40) (a) Archibald, J. L.; Walker, D. M.; Markovac, A.; Macdonald, S. F. *Can. J. Chem.* **1966**, *44*, 345. Barton, D. H. R.; Zard, S. *J. Chem. Soc., Chem. Commun.* **1985**, 1098. (b) Sessler, J. L.; Johnson, M. R.; Creager, S. E.; Fettinger, J. C.; Ibers, J. A. *J. Am. Chem. Soc.* **1990**, *112*, 9310. Sessler, J. L.; Hugdahl, J.; Johnson, M. R. *J. Org. Chem.* **1986**, *51*, 2838.

4.24 (q, 4H, $CO_2C\mathit{H}_2CH_3$), 4.05 (t, 1H, $C\mathit{H}CH_2CH_3$), 2.72 (q, 4H, C-4 $C\mathit{H}_2CH_3$), 2.06 (p, 2H, $CHC\mathit{H}_2CH_3$), 1.93 (s, 6H, CH_3), 1.25 (t, 6H, $CO_2CH_2C\mathit{H}_3$), 1.09 (t, 6H, $CH_2C\mathit{H}_3$), 0.88 (t, 3H, $CHCH_2C\mathit{H}_3$). ^{13}C-NMR ($CDCl_3$): δ 8.69, 12.35, 14.32, 14.97, 18.53, 26.45, 35.93, 59.79, 116.36, 116.89, 134.02, 134.16, 162.05. MS, *m/z* (relative intensity, %): 402 (M^+, 100), 374 (14), 373 (57), 327 (100). HRMS, *m/z*: calcd for $C_{23}H_{34}N_2O_4$, 402.2518; found, 402.2521. Anal. Calcd for $C_{23}H_{34}N_2O_4$: C, 68.63; H , 8.51; N, 6.96. Found: C, 68.72; H, 8.48; N, 6.98.

Step 2. 1,1-Bis(4-ethyl-3-methylpyrrol-2-yl)propane. The above diester (8 g, 19.8 mmol) was suspended in ethylene glycol (200 mL), aqueous sodium hydroxide (40 mL of 4 N) was added, and the mixture was heated at 190 °C for 2 h. The hot mixture was poured onto ice (500 g) and extracted with benzene. The organic layer was washed with water, dried over anhydrous sodium sulfate, and concentrated in vacuo to yield 4.6 g (90%) as a light brown oil. The residual dark brown oil was found by NMR spectroscopy to be the crude product. This product was not purified but instead was used directly in the next reaction step. ^1H-NMR ($CDCl_3$): δ 7.62 (br s, NH), 6.46 (d, 2H, pyrrole α-H), 4.08 (t, $C\mathit{H}CH_2CH_3$), 2.57 (q, 2H, $CHC\mathit{H}_2CH_3$), 2.09 (s, 6H, CH_3), 2.05 (p, $CHC\mathit{H}_2CH_3$), 1.26 (t, 3H, C-4 $CH_2C\mathit{H}_3$), 1.26 (t, 3H, C-4 $CH_2C\mathit{H}_3$).

Step 3. $H_2$10. 1,1-Bis(4-ethyl-3-methylpyrrol-2-yl)propane (4.6 g, 17.8 mmol) was dissolved in dry dichloromethane (800 mL). Dry trichloroacetic acid (45.6 g, 280 mmol) was added, followed by trimethyl orthoformate (19.4 g, 182,8 mmol), and the mixture was refluxed for 40 h, shielded from ambient lighting under nitrogen. After 40 h, 1,4-benzoquinone (2,4 g, 22.1 mmol) was added and the solution was refluxed for 3 h. The reaction mixture was cooled, washed with aqueous sodium carbonate and water, and dried over anhydrous sodium sulfate, and the solution was concentrated *in vacuo*. The resulting residue was purified via column chromatography, eluting with chloroform, and recrystallization from CH_2Cl_2/CH_3OH yielded a dark purple powder (0.88 g, 164 mmol) in 18.5% yield. Mp: 255−257 °C. UV/vis (CH_2Cl_2), λ_{max}, nm (ϵ, M^{-1} cm^{-1}): 412 (137 200), 514 (12 000), 546 (3100), 584 (4250), 642 (2900). ^1H-NMR ($CDCl_3$): δ −1.67 (br s, 2H, NH), 1.89 (t, 12H, pyrrole $CH_2C\mathit{H}_3$), 1.95 (t, 6H, meso-$CH_2C\mathit{H}_3$), 3.65 (s, 12H, pyrrole $C\mathit{H}_3$), 4.13 (q, 8H, pyrrole $C\mathit{H}_2CH_3$), 5.12 (q, 4H, meso-$C\mathit{H}_2CH_3$), 10.10 (s, 2H, meso). MS, *m/z* (relative intensity, %): 534 (M^+, 56), 532 (21), 519 (30), 505 (100). HRMS, *m/z*: calcd for $C_{36}H_{46}N_4$, 534.3725; found, 534.3725. Anal. Calcd for $C_{36}H_{46}N_4\cdot H_2O$: C, 76.02; H, 8.51; N, 9.85. Found: C, 75.87; H, 8.19; N, 9.82.

(b) Ni10. This compound was prepared from **$H_2$10** by reaction with nickel acetate. Mp: 284−285 °C. UV/vis (CH_2Cl_2) λ_{max}, nm (ϵ, M^{-1} cm^{-1}): 418 (146 200), 548 (10 600), 580 (5850). ^1H-NMR ($CDCl_3$): δ 0.76 (t, 6H, meso-$CH_2C\mathit{H}_3$), 1.67 (t, 12H, pyrrole $CH_2C\mathit{H}_3$), 3.69 (s, 12H, $C\mathit{H}_3$), 3.71 (q, 8H, pyrrole $C\mathit{H}_2CH_3$), 4.46 (q, 4H, meso-$C\mathit{H}_2CH_3$), 9.12 (s, 2H, m-H). ^{13}C-NMR ($CDCl_3$): δ 145.39, 140.51, 137.18, 136.64, 116.04, 96.06, 25.71, 19.49, 18.62, 17,31, 15, 76. MS, *m/z* (relative intensity, %): 591 (M^+, 100), 575 (29), 561 (79). HRMS, *m/z*: calcd for $C_{36}H_{44}N_4Ni$, 590.2919; found, 590.2902. Anal. Calcd for $C_{36}H_{44}N_4Ni\cdot H_2O$: C, 70.94; H, 7.61; N, 9.19. Found: C, 71.08; H, 7.45; N, 9.08.

(c) Zn10. This compound was prepared from **$H_2$10** by reaction with zinc acetate. Mp: >300 °C. UV/vis (CH_2Cl_2) λ_{max}, nm (ϵ, M^{-1} cm^{-1}): 418 (210 000), 518 sh, 548 (14 600). ^1H-NMR ($CDCl_3$): δ 1.53 (br s, 12H, pyrrole $CH_2C\mathit{H}_3$), 1.79 (t, 6H, meso-$CH_2C\mathit{H}_3$), 3.63 (s, 12H, $C\mathit{H}_3$), 4.04 (q, 8H, pyrrole $C\mathit{H}_2CH_3$), 5.16 (q, 4H, meso-$C\mathit{H}_2CH_3$), 9.93 (s, 2H, m-H). MS, *m/z* (relative intensity, %): 596 (M^+, 30), 571 (42), 569 (62), 567 (100). HRMS, *m/z*: calcd for $C_{36}H_{44}N_4Zn$, 596.2857; found, 596.2830. Anal. Calcd for $C_{36}H_{44}N_4Zn$: C, 72.32; H, 7.41; N, 9.37. Found: C, 71.98; H, 7.54; N, 9.57.

(d) $H_2$13. 2,8′-Dibutyl-3,7-dimethyldipyrrylmethane[40b] (2 g, 6.98 mmol) and freshly distilled 4-pyridinecarboxaldehyde (0.748 g, 6.98 mmol) were dissolved in methanol (700 mL), and the solution was deaerated with argon. Trifluoroacetic acid (0.55 mL, 6.98 mmol) was added, and the solution was stirred overnight at room temperature under Ar. 2,3-Dichloro-5,6-dicyano-1,4-benzoquinone (DDQ; 2.37 g, 10.5 mmol) dissolved in 100 mL of THF was added, and the resulting solution was stirred for an additional 4 h. The solvent was removed in vacuo, the residue was dissolved in dichloromethane, and the solution was washed with saturated sodium bicarbonate solution and water, dried over anhydrous sodium sulfate, and concentrated under reduced pressure. The resulting solid was purified on a silica gel column, eluting with 1% CH_3OH in CH_2Cl_2. Two fractions were obtained; the major, second band was collected, concentrated, and crystallized by addition of methanol, yielding dark red-purple crystals (1.08 g, 1.45 mmol, 41.5%). Mp: >300 °C. UV/vis (CH_2Cl_2) λ_{max}, nm (ϵ, M^{-1} cm^{-1}): 406 (181 000), 506 (15 300), 538 (5800), 574 (6400), 624 (1800). ^1H-NMR ($CDCl_3$): δ −2.42 (br s, 2H, NH), 1.10 (t, 12H, $CH_2CH_2CH_2C\mathit{H}_3$), 1.75 (m, 8H, $CH_2CH_2C\mathit{H}_2CH_3$), 2.16 (p, 8H, $CH_2C\mathit{H}_2CH_2CH_3$), 2.50 (s, 12H, $C\mathit{H}_3$), 3.97 (t, 8H, $C\mathit{H}_2CH_2CH_2CH_3$), 8.04 (d, 4H, pyridine β-H), 9.01 (d, 4H, pyridine α-H), 10.26 (s, 2H, m-H). MS, *m/z* (relative intensity, %): 744 (M^+, 7), 668 (100), 624 (25). HRMS, *m/z*: calcd for $C_{50}H_{60}N_6$, 744.4879; found, 744.4851. Anal. Calcd for $C_{50}H_{60}N_6\cdot H_2O$: C, 78.70; H, 8.19; N, 11.01. Found: C, 78.68; H, 7.99; N, 10.97. On the basis of ^1H-NMR and mass spectral data, the leading band was determined to be 2,8,12,18-tetrabutyl-3,7,13,17-tetramethyl-5-(4-pyridyl)porphyrin.

(e) Ni13. This compound was prepared in 90% yield from **$H_2$13** by reaction with nickel acetylacetonate. Mp: 280−281 °C. UV/vis (CH_2Cl_2) λ_{max}, nm (ϵ, M^{-1} cm^{-1}): 406 (181 000), 528 (11 500), 564 (17 000). ^1H-NMR ($CDCl_3$): δ 1.04 (t, 12H, $CH_2CH_2CH_2C\mathit{H}_3$), 1.61 (m, 8H, $CH_2CH_2C\mathit{H}_2CH_3$), 1.98 (p, 8H, $CH_2C\mathit{H}_2CH_2CH_3$), 2.26 (s, 12H, $C\mathit{H}_3$), 3.65 (t, 8H, $C\mathit{H}_2CH_2CH_2CH_3$), 7.85 (d, 4H, pyridine β-H), 8.92 (d, 4H, pyridine α-H), 9.46 (s, 2H, m-H). ^{13}C-NMR ($CDCl_3$): δ 14.07, 15.61, 23.11, 25.98, 34.95, 96.89, 113.47, 128.47, 138.25, 139.32, 139.64, 144.80, 148.94, 149.42; MS, *m/z* (relative intensity, %): 800 (M^+, 100), 757 (11), 723 (40). HRMS, *m/z*: calcd for $C_{50}H_{58}N_6Ni$, 800.4076; found, 800.4076. Anal. Calcd for $C_{50}H_{58}N_6Ni\cdot 2.5H_2O$: C, 70.92; H, 7.50; N, 9.92. Found: C, 71.14; H, 7.39; N, 9.73.

X-ray Crystallography. Single crystals of the listed compounds were grown from dichloromethane/methanol. The crystals were immersed in hydrocarbon oil, and a single crystal was selected, mounted on a glass fiber, and placed in the low-temperature N_2 stream.[41a] Used for data collection was either a Siemens R3m/V automatic diffractometer equipped with a graphite monochromator and with a locally modified low-temperature device or a Siemens P4 instrument equipped with a Siemens LT device and a Siemens rotating anode, operated at 50 kV and 300 mA. Cell parameters for the structures measured with Mo Kα radiation were determined from 20−30 reflections in the range $20° \leq 2\theta \leq 30°$; for structures measured with Cu Kα radiation, the range $40° \leq 2\theta \leq 60°$ was used. Two standard reflections were measured every 198 reflections and showed only statistical variation in intensity during all data collection (<2% intensity change). The intensities were corrected for Lorentz and polarization effects. In all cases, an absorption correction was applied using the program XABS;[41b] extinction effects were disregarded. The free-base porphyrin structures were solved using direct methods, while the Ni(II) porphyrin structures were solved via Patterson syntheses followed by subsequent structure expansion using the SHELXTL PLUS program system.[41c] Refinements were carried out by full-matrix least-squares procedures on $|F|$ using the same program system. The function minimized was $\sum w(F_o - F_c)^2$. Hydrogen atoms were included at calculated positions by using a riding model (C−H distance 0.96 Å, N−H distance 0.9 Å). All calculations were carried out on a Vax-station 3200. All non-hydrogen atoms were refined with anisotropic parameters. In the case of **Ni10**, only the nickel and nitrogen atoms and the peripheral ethyl and methyl carbon atoms were refined with anisotropic thermal parameters. The refinement of the structure of **Ni12** gave unsatisfactory final *R* values because of poor crystal quality and a low-intensity data set and high thermal motion of some of the side chain atoms in the structure. The ethyl ester side chain in **Ni19** was found to be disordered. The ethyl carbon atoms [C(104) and C(105)] were refined with two split positions with occupancies of 0.55 and 0.45.

Further details of the crystal data and structure solutions and refinements are listed in Table 1 and in the Supporting Information.

---

(41) (a) Hope, H. *ACS Symp. Ser.* **1987**, *357*, 257. (b) Hope, H.; Moezzi, B. *XABS*; University of California: Davis, CA, 1987. (c) *SHELXTL PLUS*; Siemens Analytical Instruments, Inc.: Madison, WI, 1990.

Table 1. Crystal Data and Data Collection and Refinement Parameters

	Ni10	**$H_2$11**	**Ni11**	**Ni12**	**$H_2$13**	**$H_2$14**	**$H_2$15**	**$H_2$16**	**Ni17**	**Ni18**	**Ni19**
empirical formula	$C_{36}H_{44}N_4Ni$	$C_{44}H_{46}N_4$	$C_{44}H_{44}N_4Ni$	$C_{48}H_{52}N_4NiO_4$	$C_{50}H_{62}N_6$	$C_{40}H_{46}N_4O{\cdot}C_6H_{14}$	$C_{41}H_{46}Cl_2N_4$	$C_{40}H_{44}N_4O_2$	$C_{44}H_{45}ClN_4NiO_5$	$C_{49}H_{50}N_4NiO$	$C_{45}H_{44}N_4NiO$
crystal size, mm	0.3 × 0.15 × 0.08	0.24 × 0.16 × 0.15	0.84 × 0.15 × 0.08	0.25 × 0.08 × 0.03	0.4x0.21 × 0.06	0.16 × 0.13 × 0.03	0.34 × 0.1 × 0.2	0.21 × 0.18 × 0.17	0.45 × 0.25 × 0.21	1.1 × 0.5 × 0.008	0.48 × 0.2 × 0.2
color, habit	red needle	red octahedron	red parallelepiped	red parallelepiped	red parallelepiped	red plate	red parallelepiped	red cube	green parallelepiped	red plate	blue parallelepiped
mol wt	591.5	630.8	687.5	807.6	747.1	685.0	665.7	612.8	804.0	785.6	715.6
space group	$P2_1/c$	$P2_1/n$	$C2/c$	$P2_1/c$	$P\bar{1}$	$P2_1/c$	$P2_1/c$	$P\bar{1}$	$P2_1/c$	$P\bar{1}$	$P2_1/n$
a, Å	24.478(3)	8.814(4)	17.778(7)	7.949(3)	8.851(3)	8.090(2)	8.596(2)	9.095(2)	13.551(12)	9.998(2)	14.209(3)
b, Å	9.816(2)	10.680(4)	19.922(12)	20.574(11)	10.177(5)	12.598(2)	12.269(3)	13.412(4)	24.956(14)	13.666(3)	19.219(5)
c, Å	25.501(4)	18.751(6)	10.517(5)	12.800(5)	12.631(6)	34.86(2)	33.030(9)	15.165(3)	12.155(8)	14.953(2)	14.802(3)
α, deg	90	90	90	90	107.68(4)	90	90	65.59(2)	90	82.41(2)	90
β, deg	90.75(2)	100.24(3)	115.03(3)	91.36(3)	92.36(3)	94.82(3)	92.42(2)	76.51(2)	108.68(6)	76.67(2)	117.26(2)
γ, deg	90	90	90	90	104.24(3)	90	90	79.62(2)	90	86.33(2)	90
V, Å^3	6186(2)	1737.1(12)	3375(3)	2092.6(15)	1042.4(8)	3540(2)	3480(1)	1631(1)	3894(5)	1969(1)	3593(1))
Z	8 (2 ind. mol.)	2	4	2	1	4	4	2	4	2	4
D_{calcd}, g·cm^{-3}	1.270	1.206	1.353	1.282	1.190	1.283	1.271	1.248	1.371	1.325	1.323
μ, mm^{-1}	1.127	0.066	1.118	1.053	0.070	0.584	1.941	0.604	0.619	1.066	1.094
radiation	Cu Kα	Mo Kα	Cu Kα	Cu Kα	Mo Kα	Cu Kα	Cu Kα	Cu Kα	Mo Kα	Cu Kα	Cu Kα
λ, Å	1.541 78	0.710 73	1.541 78	1.541 78	0.710 73	1.541 78	1.541 78	1.541 78	0.710 73	1.541 78	1.541 78
diffractometer	Siemens P4/RA	Siemens R3m/V	Siemens P4/RA	Siemens P4/RA	Siemens R3m/V	Siemens P4/RA	Siemens P4/RA	Siemens P4/RA	Siemens R3m/V	Siemens P4/RA	Siemens P4/RA
T, K	126	130	126	126	130	126	126	126	130	126	126
$2\theta_{\max}$, deg	108.5	55	108.5	108.5	55	108.5	112	108.5	55	108.5	114
no. of indep reflns	7493	3976	2031	2562	4570	4349	4541	4003	8464	4814	4727
no. of obs reflns	5867	2164	1824	1756	2793	3099	3460	3125	5321	3818	3942
crit for obs reflns	$F > 3.5\sigma(F)$	$F > 4.0\sigma(F)$	$F > 4.0\sigma(F)$	$F > 6.0\sigma(F)$	$F > 4.0\sigma(F)$	$F > 3.5\sigma(F)$	$F > 4.0\sigma(F)$	$F > 3.5\sigma(F)$	$F > 4.0\sigma(F)$	$F > 4.0\sigma(F)$	$F > 4.0\sigma(F)$
no. of parameters	529	217	223	260	253	433	424	415	496	524	460
R	0.055	0.059	0.072	0.133	0.063	0.061	0.052	0.07	0.058	0.059	0.047
R_{w}	0.062	0.068	0.111	0.166	0.084	0.073	0.065	0.096	0.054	0.081	0.07
S	1.54	1.12	0.21	4.16	1.05	1.48	1.38	1.80	1.34	1.77	1.23

Table 2. Selected Structural Parameters for Geometrically Equivalent Positions of Porphyrins $\mathbf{H_2 11}$, $\mathbf{H_2 13}$, **Ni11**, and **Ni10**

	$\mathbf{H_2 11}$		$\mathbf{H_2 13}$		**Ni11**		**Ni10**			
							molecule 1		molecule 2	
	meso-H	meso-R	meso-H	meso-R	meso-H	meso-R	meso-H	meso-R	meso-H	meso-R
Displacements, Å										
24 core atoms[a]	0.04		0.03		0.21		0.37		0.37	
N_4 plane[a]	0		0		0.10		0.01		0.01	
Ni[b]					0 (0)		0.02 (0.02)		0.01 (0.01)	
C_m[b]	0.08 (0.01)	0.11 (0.08)	0.11 (0.01)	0.09 (0.03)	0 (0)	0.13 (0.11)	0.70 (0.71)	0.85 (0.85)	0.68 (0.71)	0.86 (0.84)
C_a[b]	0.07 (0.03)	0.04 (0.03)	0.08 (0.02)	0.08 (0.03)	0.20 (0.19)	0.18 (0.17)	0.42 (0.43)	0.44 (0.44)	0.41 (0.44)	0.45 (0.43)
C_b[b]	0.13 (0.05)	0.10 (0.07)	0.14 (0.03)	0.16 (0.04)	0.37 (0.37)	0.38 (0.38)	0.32 (0.33)	0.26 (0.25)	0.29 (0.31)	0.29 (0.27)
Bond Lengths and Distances, Å										
core size	2.086		2.094		1.957		1.899		1.903	
N−N separation	3.159	2.727	3.207	2.692	2.833	2.706	2.731	2.641	2.736	2.646
Ni−N					1.957(3)		1.900(4)		1.903(3)	
$N-C_a$	1.374(3)	1.373(3)	1.362(4)	1.373(2)	1.377(4)	1.393(4)	1.380(5)	1.386(6)	1.375(6)	1.386(6)
C_a-C_b	1.454(4)	1.461(4)	1.451(4)	1.467(4)	1.437(4)	1.459(4)	1.436(6)	1.461(6)	1.436(6)	1.452(6)
C_a-C_m	1.387(4)	1.408(4)	1.389(4)	1.412(4)	1.364(4)	1.384(4)	1.377(6)	1.400(6)	1.381(6)	1.398(6)
C_b-C_b	1.359(4)		1.362(4)		1.349(4)		1.350(6)		1.363(6)	
C_b-CH_x	1.503(4)	1.504(4)	1.501(5)	1.506(5)	1.507(4)	1.507(5)	1.509(6)	1.510(7)	1.503(6)	1.510(7)
C_m-C		1.498(4)		1.494(4)		1.506(4)		1.512(6)		1.522(6)
Bond Angles, deg										
N−Ni−N adj					92.8(1)	87.5(1)	91.2(2)	88.1(2)	92.0(2)	88.1(2)
N−Ni−N opp					174.1(1)		178.8(2)		179.2(2)	
$Ni-N-C_a$					125.0(2)	130.3(2)	125.7(3)	128.2(3)	125.6(3)	128.3(3)
$N-C_a-C_m$	127.4(3)	123.0(2)	127.8(3)	122.4(3)	125.4(3)	123.9(3)	123.6(4)	123.3(4)	124.1(4)	123.1(4)
$N-C_a-C_b$	108.5(2)	108.5(2)	109.1(3)	108.6(3)	111.2(3)	109.9(3)	110.2(4)	109.2(4)	110.5(4)	109.4(4)
C_a-N-C_a	108.3(2)		108.3(3)		104.9(2)		106.0(3)		106.1(3)	
$C_a-C_m-C_a$	131.7(3)	123.8(2)	132.5(3)	123.7(3)	125.6(3)	122.9(3)	124.4(4)	119.6(4)	123.9(4)	120.3(4)
$C_a-C_b-C_b$	107.9(2)	106.8(2)	107.5(3)	106.6(3)	107.2(3)	106.8(3)	107.6(4)	106.9(4)	106.9(4)	107.0(4)
$C_m-C_a-C_b$	124.1(2)	128.4(2)	123.3(3)	129.0(3)	123.2(3)	126.2(3)	125.5(4)	127.1(4)	124.6(4)	127.2(4)
$C_a-C_b-CH_x$	124.8(2)	129.2(3)	123.7(3)	129.1(3)	123.9(2)	129.9(2)	124.0(4)	128.7(4)	125.0(4)	129.0(4)
$C_b-C_b-CH_x$	127.2(3)	124.0(3)	128.9(3)	124.3(3)	128.9(3)	123.4(3)	128.2(4)	124.2(4)	128.0(4)	123.8(4)

[a] Mean deviation of all atoms in least-squares plane. [b] Deviations from N_4 plane; numbers in parentheses are deviations from the least-squares plane of the 24 core atoms.

Results and Discussion

Crystal Structures. Selected structural parameters for the porphyrins investigated are given in Tables 2−4. 5,15-Diaryl-substituted porphyrins of type **11** were first studied in order to allow a comparison with the 5,15-dialkyl-substituted porphyrins of type **9** studied earlier.[35] The molecular structure of the free-base porphyrin $\mathbf{H_2 11}$ is shown in Figure 1. The porphyrin is located on a crystallographic inversion center. The molecular structure is characterized by a relatively planar macrocycle core. The overall degree of distortion in the macrocycle is small with an average deviation of the 24 core atoms from their least-squares plane of 0.04 Å and angles between the pyrrole planes and the plane of the four nitrogens (N_4 plane) of only 2.6 and 4.3°. Due to the crystallographically imposed symmetry, the macrocycle is slightly folded along the C(5)-C(15) axis. The largest deviations are observed for the C_b atoms, which have deviations of up to 0.16 Å.

The general trends in bond lengths and bond angles for the pyrrole rings and the unsubstituted meso positions in $\mathbf{H_2 11}$ are similar to those of other free-base porphyrins like TPP ($\mathbf{H_2 2}$) or OEP ($\mathbf{H_2 1}$).[5,42] However, a closer inspection reveals significant differences between the meso-H and meso-phenyl quadrants of the molecule (Table 2). The C_a-C_m bond lengths are elongated [1.408(4) vs 1.387(4) Å] while the $N-C_a-C_m$ [123.0(2) vs 127.4(3)°] and $C_a-C_m-C_a$ [123.8 vs 131.7(3)°] bond angles are narrowed in the meso-phenyl quadrants. The $C_m-C_a-C_b$ angles are also widened in the meso-phenyl quadrant [128.4(2)°] compared to the meso-H quadrant [124.1(2)°], and significant differences are observed between the C_a-C_b-CH and C_b-C_b-CH angles of the two quadrants. A comparison with the respective structures of free-base OEP[42a] and TPP[42b] reveals that the differences between the two quadrants cannot be attributed solely to a substitution effect. The differences are significantly larger than those observed between OEP and TPP and, as discussed later, can be readily explained in terms of distortions which reduce steric interactions between the meso-phenyl and neighboring pyrrole groups. In addition to differences in the bond lengths and angles, a unique structural pattern is observed with regard to the orientation of the meso-phenyl groups. With respect to the N_4 plane, the meso carbons are displaced by about 0.1 Å above and below the plane and the phenyl ipso carbons are oriented above and below the N_4 plane by 0.34 Å, respectively, giving an anti orientation of the phenyl groups with respect to the molecular plane. The phenyl rings are almost orthogonal to the N_4 plane and make an angle of 85.4°.

While the out-of-plane distortions in $\mathbf{H_2 11}$ are not very large, there is clearly significant in-plane distortion of the macrocycle, as evidenced by a change from the typical square geometry in the porphyrin to a rectangular elongated core characterized by the relevant N···N separation along the two molecular axes (Table 2). A similar effect was previously observed for $\mathbf{H_2 9}$.[35] In $\mathbf{H_2 11}$, the N···N separation along the 5,15-axis is 3.159 Å, while the N···N separation along the 10,20-axis is 2.727 Å ($\Delta_{N\cdots N} = 0.43$ Å). Typically, porphyrins exhibit similar N···N separations along both axes on the order of 2.6−2.8 Å. This asymmetry in the macrocycle is mirrored in the relevant $C_a-C_m-C_a$ bond angles. While the average bond angle in the meso-phenyl quadrant is 123.8(2)°, this angle is considerably widened

---

(42) (a) Lauher, J. W.; Ibers, J. A. *J. Am. Chem. Soc.* **1973**, *95*, 5148. (b) Silvers, S. J.; Tulinsky, A. *J. Am. Chem. Soc.* **1967**, *89*, 3331. (c) Codding, P. W.; Tulinsky, A. *J. Am. Chem. Soc.* **1972**, *94*, 4151.

Table 3. Displacements (Å) along the Lowest-Frequency [Minimal Basis Set (min)] and Second-Lowest-Frequency [Extended Basis Set (ext)] Out-of-Plane and In-Plane Normal Coordinates of the Macrocycle for Nickel(II) Metalloporphyrin X-ray Crystal Structures, along with the Observed (D_{obs}) and Simulated (D_{sim}) Total Distortions and the Mean Simulated Errors (δ)

					mode					
porphyrin	D_{obs}^{oop}	basis	D_{sim}^{oop}	$\bar{\delta}_{oop}$	B_{2u}	B_{1u}	A_{2u}	$E_{g(x)}$	$E_{g(y)}$	A_{1u}
Ni10	2.190	min	2.182	0.027	−0.453	2.133	0.074	0.026	−0.027	0.010
		ext	2.189	0.007	−0.452	2.133	0.067	0.025	−0.027	0.010
					0.057	0.046	−0.156	−0.022	0.012	0.000
Ni10	2.149	min	2.143	0.025	0.260	2.127	0.022	−0.057	−0.019	−0.003
		ext	2.149	0.007	0.260	2.127	0.016	−0.056	−0.019	−0.003
					−0.010	0.036	−0.148	0.009	0.004	−0.009
Ni11	1.219	min	1.211	0.023	−1.192	0.000	0.000	0.154	0.154	0.000
		ext	1.219	0.005	−1.193	0.000	0.000	0.151	0.151	0.000
					−0.049	0.000	0.000	−0.090	−0.090	−0.012
Ni12	0.123	min	0.105	0.010	0.000	0.000	0.000	0.008	0.104	0.000
		ext	0.117	0.006	0.000	0.000	0.000	0.009	0.103	0.000
					0.000	0.000	0.000	0.014	−0.051	0.000
Ni17	2.070	min	2.062	0.027	−0.053	2.023	0.137	−0.27	−0.251	0.011
		ext	2.068	0.012	−0.053	2.023	0.132	−0.268	−0.247	0.011
					−0.004	0.017	−0.112	0.05	0.110	0.011
Ni18	3.083	min	3.078	0.026	2.806	−1.234	0.199	0.037	0.195	−0.035
		ext	3.083	0.007	2.803	−1.234	0.197	0.040	0.193	−0.035
					−0.140	0.007	−0.037	0.068	−0.054	0.000
Ni19	2.183	min	2.172	0.032	−1.033	−1.883	0.172	−0.147	0.228	0.017
		ext	2.182	0.010	−1.032	−1.883	0.165	−0.143	0.225	0.017
					0.050	−0.021	−0.157	0.084	−0.100	−0.008

					mode					
porphyrin	D_{obs}^{ip}	basis	$D_{sim,1}^{ip}$	$\bar{\delta}_{ip}$	B_{2g}	B_{1g}	$E_{u(x)}$	$E_{u(y)}$	A_{1g}	A_{2g}
Ni10	0.654	min	0.559	0.061	−0.109	−0.010	−0.012	0.012	−0.548	−0.018
		ext	0.632	0.025	−0.109	−0.010	−0.012	0.012	−0.547	−0.019
					−0.017	−0.012	−0.006	−0.012	0.279	−0.093
Ni10	0.633	min	0.544	0.058	−0.090	0.009	−0.009	−0.028	−0.536	0.000
		ext	0.615	0.024	−0.090	0.009	−0.009	−0.028	−0.535	0.000
					−0.036	0.006	0.013	0.027	0.278	0.050
Ni11	0.295	min	0.264	0.024	−0.193	0.000	0.034	−0.034	−0.173	0.000
		ext	0.288	0.013	−0.194	0.000	0.034	−0.034	−0.173	0.000
					−0.112	0.000	−0.014	0.014	−0.024	0.000
Ni12	0.263	min	0.190	0.031	−0.175	−0.010	0.000	0.000	−0.064	0.032
		ext	0.247	0.015	−0.176	−0.010	0.000	0.000	−0.064	0.032
					−0.156	0.019	0.000	0.000	−0.020	0.000
Ni17	0.633	min	0.522	0.060	0.010	−0.035	−0.053	−0.151	−0.496	0.006
		ext	0.604	0.032	0.011	−0.035	−0.053	−0.15	−0.495	0.006
					0.129	0.008	0.000	0.073	0.266	−0.015
Ni18	0.847	min	0.756	0.071	−0.008	0.131	−0.003	0.025	−0.744	−0.009
		ext	0.818	0.041	−0.009	0.132	−0.004	0.025	−0.745	−0.012
					−0.052	0.012	−0.017	0.042	−0.074	−0.294
Ni19	0.601	min	0.490	0.057	−0.092	−0.014	−0.094	0.031	−0.471	−0.004
		ext	0.577	0.029	−0.093	−0.014	−0.093	0.031	−0.471	−0.003
					−0.161	−0.022	0.040	−0.002	0.198	0.160

[a] For further details of the model used, see: Jentzen, W.; Song, X.-Z.; Shelnutt, J. A. *J. Phys. Chem.*, in press.

in the meso-H quadrant [131.7(3)°] and the C_a-C_m bond lengths are elongated in the H quadrant [1.408(4) Å vs 1.374(3) Å]. Thus, like **H₂9**, **H₂11** experiences considerable steric strain from the peripheral substituents which is relieved in the major part by in-plane distortion of the macrocycle. If no steric strain would have been present, neither out-of-plane distortion (which is minimal) nor in-plane rotation (which is significant) would have been observed.

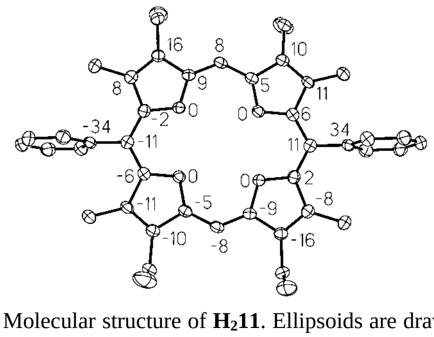

Figure 1. Molecular structure of **H₂11**. Ellipsoids are drawn for 50% occupancy, and hydrogen atoms have been omitted for clarity. Numbers give the deviations of the macrocycle atoms from the least-squares plane of the four nitrogen atoms (Å × 10^2).

A similar essentially planar conformation was observed in the molecular structure of **H₂13** (Figure 2). Instead of meso-phenyl groups, this compound bears 4-pyridyl groups and has *n*-butyl substituents at the 2,8,12,18-positions; selected structural data and geometrical features are listed in Table 2. Like **H₂12**, the molecule has a crystallographically imposed inversion point. The trends and differences in the meso-H and meso-aryl quadrants are the same as those described for **H₂11**. The aryl group is tilted 4° against the N_4 plane, and the pyrrole rings are tilted 4.9° against the N_4 plane. The macrocycle is again folded along the C(5)−C(15) axis and shows significant but small deviations from planarity and has a similar anti orientation of the meso-aryl groups. The two N···N axes are clearly inequivalent with N···N distances of 2.692 and 3.207 Å, respectively.

The crystallographic data reported for **H₂11** and **H₂13** in this paper, together with the similar structure reported for **H₂9**,[35] suggest that in-plane distortion along the 5,15-axis is a viable

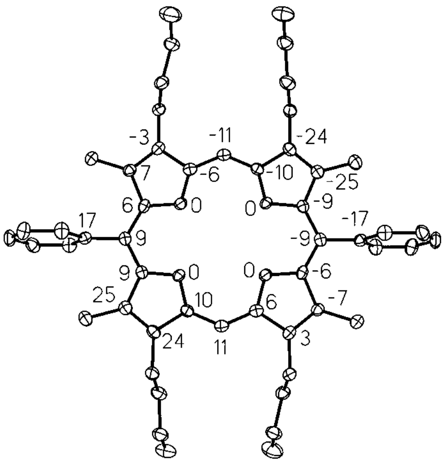

Figure 2. Molecular structure of **H$_2$13**. Ellipsoids are drawn for 50% occupancy, and hydrogen atoms have been omitted for clarity. Numbers give the deviations of the macrocycle atoms from the least-squares plane of the four nitrogen atoms (Å × 10^2).

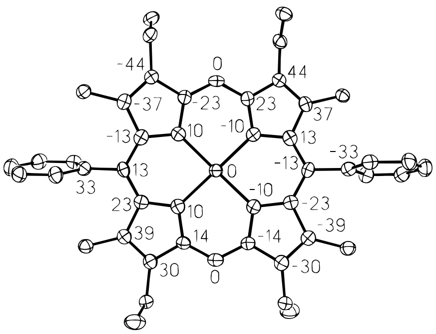

Figure 3. Molecular structure of **Ni11**. Ellipsoids are drawn for 50% occupancy, and hydrogen atoms have been omitted for clarity. Numbers give the deviations of the macrocycle atoms from the least-squares plane of the four nitrogen atoms (Å × 10^2).

alternative to out-of-plane distortion for relieving peripheral steric strain in these systems. This view was supported by a review of 5,15-diarylporphyrins in the literature.[43ab] For example, a similar elongation along the aryl−aryl axis and a slight anti orientation of the aryl rings were observed in two 5,15-diphenyloctaalkylporphyrins where the phenyl rings were covalently linked in the ortho positions by alkyl chains and a quinone spacer group to make a “strapped-type” porphyrin.[43a] The differences in the N···N distances were similar in both structures: $\Delta_{N\cdots N} = 0.43$ Å [3.14 Å (C(5)−C(15) axis) and 2.71 Å (C(10)−C(20) axis)], and $\Delta_{N\cdots N} = 0.44$ Å [3.16 Å (C(5)−C(15) axis) and 2.72 Å (C(10)−C(20) axis)]. Structures determined by Gunter et al. in which the meso-phenyl groups were connected in the ortho positions by ether bridges showed either nonplanar or planar macrocycle conformations depending on the length of the strap.[43b] Rectangular porphyrin cores have also been noted in 5-substituted octaalkylporphyrins,[24,31b] although the degree of in-plane distortion in these systems was less than that observed for the 5,15-substituted porphyrins [e.g., 2.96 Å along the C(5)−C(15) axis and 2.83 Å along the C(10)−C(20) axis], giving $\Delta_{N-N} = 0.13$ Å.[24a]

In order to study metal effects in the 5,15-substituted porphyrins, the nickel(II) complex of **11** was also prepared and structurally analyzed (Figure 3). The molecular structure of **Ni11** is characterized by a crystallographically required 2-fold axis which passes through the Ni, C(10), and C(20) atoms. The structure is quite different from the corresponding free-base **H$_2$11**. The macrocycle conformation is nonplanar, as evidenced by an average deviation of the macrocycle atoms from the 24-core-atom plane of 0.21 Å, and the conformation can be best described as a shallow saddle.[22] The maximum distortions observed are on the order of 0.4 Å for the C_b atoms; this is slightly smaller than those observed in the tetragonal form of NiOEP,[44a] which is characterized by S_4 ruffling.[22] While the out-of-plane distortion is significant in **Ni11**, only small differences were found for the N···N separations [2.833 and 2.706, $\Delta_{N\cdots N} = 0.13$ Å] (Table 2), indicating that the in-plane distortion is less pronounced than that seen for **H$_2$11**. As expected, the average Ni−N bond length in **Ni11** [1.957(3) Å] is longer than that seen in severely saddled dodecasubstituted Ni(II) porphyrins (1.902−1.922 Å).[15c,20c] The phenyl rings deviate considerably from an orthogonal orientation with respect to the macrocycle plane (90° − 78.6° = 11.4°).

The distortions of the substituted and unsubstituted C_m atoms were nonequivalent, with the unsubstituted C_m atoms showing no deviation from the N_4 plane while the phenyl-substituted ones were displaced by 0.13 Å alternatively above and below the mean plane. This leads to a deviation of the phenyl C_i atoms from the macrocycle plane by 0.33 Å. Owing to the inversion center, an anti orientation of the aryl groups with tilting above and below the macrocycle plane was again observed. A comparison of the relevant bond lengths and angles (Table 2) for the meso-aryl and meso-H quadrants revealed the same differences seen for **H$_2$11**, although the magnitude of the differences was significantly smaller in **Ni11**. Thus, it appears that the presence of the central metal leads to a redistribution of the conformational strain energy within the macrocycle. Note that large differences were observed for the N−Ni−N (adj) angle, which was smaller by 5° in the meso-phenyl quadrant, and in the Ni−N−C_a angle, which is about 5° larger in the meso-phenyl quadrant.

Recently, it was shown that the nonplanar distortions encountered in the crystal structures of porphyrins correspond to distortions along the lowest-energy vibrational modes of the porphyrin macrocycle.[45] Decomposition of the static nonplanar distortions seen in the crystal structures into contributions from the lowest-energy normal modes indicates the amount of each type of nonplanar distortion present, although generally only four of the out-of-plane normal modes are of sufficiently low energy to make a significant contribution [the B_{2u} mode (saddle disortion), the B_{1u} mode (ruffle distortion), the A_{2u} mode (doming), and the E_g mode (wave distortion)—see Figure 4]. The crystal structures of **Ni11** and the other nickel porphyrins used in this study were subjected to this decomposition procedure. The results of these calculations are summarized in Table 3.

Excellent agreement was obtained between the observed and fitted total out-of-plane distortions for **Ni11** and the other nickel porphyrins investigated in this study, especially when the expanded basis set was employed. The decomposition process revealed that the nonplanar conformation of **Ni11** consisted

---

(43) (a) Krieger, C.; Dernbach, M.; Voit, G.; Carell, T.; Staab, H. A. *Chem. Ber.* **1993**, *126*, 811. (b) Gunter, M. J.; Hockless, D. C. R.; Johnston, M. R.; Skelton, B. W.; White, A. H. *J. Am. Chem. Soc.* **1994**, *116*, 4810. (c) Staab, H. A.; Krieger, C.; Anders, C.; Rückemann, A. *Chem. Ber.* **1994**, *127*, 231.

(44) (a) Meyer, E. F., Jr. *Acta Crystallogr.* **1972**, *B28*, 2162. (b) Cullen, D. L.; Meyer, E. F., Jr. *J. Am. Chem. Soc.* **1974**, *96*, 2095. (c) Alden, R. G.; Crawford, B. A.; Doolen, R.; Ondrias, M. R.; Shelnutt, J. A. *J. Am. Chem. Soc.* **1989**, *111*, 2070. (d) Brennan, T. D.; Scheidt, W. R.; Shelnutt, J. A. *J. Am. Chem. Soc.* **1988**, *110*, 3919.

(45) Jentzen, W.; Hobbs, J. D.; Simpson, M. C.; Taylor, K. K.; Ema, T.; Nelson, N. Y.; Medforth, C. J.; Smith, K. M.; Veyrat, M.; Mazzanti, M.; Ramasseul, R.; Marchon, J.-C.; Takeuchi, T.; Goddard, W. A., III; Shelnutt, J. A. *J. Am. Chem. Soc.* **1995**, *117*, 11085.

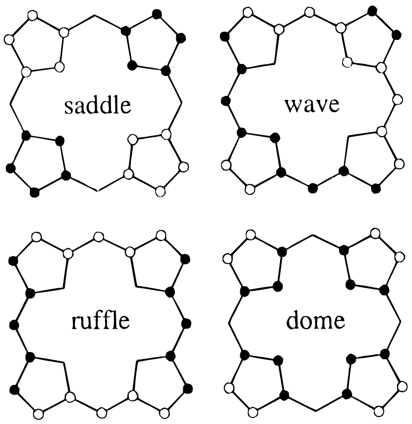

Figure 4. The four symmetrical nonplanar distortions commonly encountered for porphyrins.[45] Circles and filled circles correspond to atoms above and below the least-squares plane of the 24 atoms of the porphyrin core, respectively, whereas atoms not represented by circles are in the plane.

mainly of a saddle distortion with some wave distortion. A comparable decomposition of the in-plane distortion for **Ni11** revealed that it was dominated by the A_{1g} (breathing) mode due to contraction of the porphyrin core around the nickel(II) atom. A similar pattern of in-plane distortion was seen for the other very nonplanar nickel(II) porphyrins investigated in this study.

The crystal structure of **Ni12** (not shown) is of marginal quality, but several general trends can be observed. The phenyl ipso carbon atoms again show an up and down displacement with respect to the N_4 plane (~0.3 Å), which is required by the crystallographic symmetry operation. However, in contrast to the structure of **Ni11**, a planar macrocycle conformation was observed. The average deviation of the macrocycle atoms from the 24-core-atom least-squares plane was only 0.02 Å, with the largest observed deviation being 0.05 Å for the substituted C_m atoms. The structure of **Ni12** therefore more closely resembles the situation found in the planar forms of NiOEP.[44b,d] This similarity is also evidenced by an average Ni−N bond length of 1.967(9) Å and an average angle of 1.5° between the N_4 plane and the planes of the individual pyrrole rings.

The different conformations seen for **Ni11** and **Ni12** show that nickel(II) 5,15-diaryloctaalkylporphyrins can adopt both planar and nonplanar conformations [a similar situation is observed for NiOEP, which adopts planar and nonplanar (ruffled) conformations in the crystalline state].[44] Interestingly, two related nickel(II) porphyrins with meso-*o*-(β-alanylamido)-phenyl[46a] and meso-*o*-(nicotinoylamino)phenyl[46b] substituents exhibited *ruffled* structures similar to the nonplanar form of NiOEP. Complexes of 5,15-diarylporphyrins with $Mo^{V}O$[47] or Zn(II)[43c,48] were essentially planar, as was the Zn(II) complex of 5,15-dinitro-OEP.[20b] The available crystal structures thus clearly indicate that metal complexes of the 5,15-diarylporphyrins are not intrinsically nonplanar.

Earlier, we reported the crystal structure of **Ni9**, where the meso-substituents were flanked by ethyl groups.[35] In order to study the influence of different flanking groups, we investigated the conformation of **Ni10**, where the meso-ethyl substituents are flanked by methyl groups. Figure 5 shows the molecular structure of **Ni10**, which crystallizes with two independent molecules per asymmetric unit. The main difference between the two independent molecules is the relative orientation of the pyrrole ethyl groups. The molecule with Ni(1) has two ethyl groups pointing to one side [C(2), C(18)] in the same direction as the meso-ethyl groups and two pointing toward the other side of the macrocycle [C(8), C(12)], while the molecule with Ni(2) has three ethyl groups [C(28), C(32), C(38)] pointing in the same direction as the meso-ethyl groups and one pointing in the other direction [C(22)]. Otherwise, the general structural characteristics of both molecules are similar.

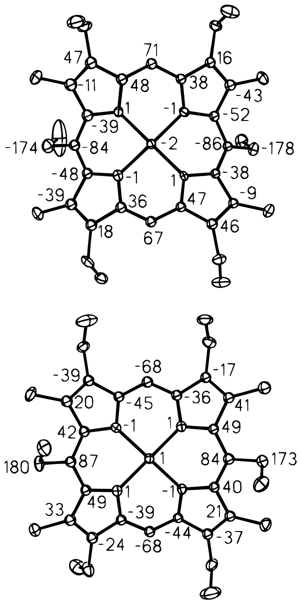

Figure 5. View of the two independent molecules in the structure of **Ni10**. Ellipsoids are drawn for 50% occupancy, and hydrogen atoms have been omitted for clarity. Numbers give the deviations of the macrocycle atoms from the least-squares plane of the four nitrogen atoms (Å × 10^2).

Decomposition of the out-of-plane distortions for the two molecules indicated only slight differences in the total distortion and how it was distributed between the normal coordinates (Table 3). The average displacements of the core atoms (0.37 Å) and the average angles of the pyrrole rings with the N_4 plane (24°) in **Ni10** were the same as those seen for **Ni9**,[35] indicating that the flanking groups have little effect on the porphyrin conformation. The similar structures seen for **Ni9** and **Ni10** suggested that, in contrast to the 5,15-diaryloctaalkylporphyrins, the 5,15-dialkyloctaalkylporphyrins were intrinsically nonplanar. This was supported by the crystal structures of iron(III)[25b] and copper(II)[28b,29] complexes of 5,15-dialkyloctaalkylporphyrins, all of which showed similar ruffled structures.

The range of structures available for the 5,15-substituted porphyrins allowed us to examine in more detail how steric repulsions between the peripheral substituents were minimized by in-plane or out-of-plane distortions. Table 5 summarizes the structural differences between substituted and unsubstituted positions within the molecule for a range of 5,15-substituted porphyrins. Note that the changes in bond angles are precisely those expected to minimize interactions between the meso-substituents and pyrrole substituents; i.e., the pyrrole subunits move away from the meso-substituents, resulting in a decrease in the $C_a-C_m-C_a$ angle, the pyrrole substituents themselves move away from the meso-substituents, resulting in an increase in the $C_a-C_b-C_x$ angle and a decrease in the $C_b-C_b-C_x$ angle, and the pyrrole rings tilt about the C_m-C_a bond, resulting in an increase in the $C_m-C_a-C_b$ angle and a corresponding decrease in the C_m-C_a-N angle. These structural differences

---

(46) (a) Woo, L. K.; Maurya, M. R.; Tolpii, C. J.; Jacobson, R. A.; Yang, S.; Rose, E. *Inorg. Chim. Acta* **1991**, *182*, 41. (b) Woo, L. K.; Maurya, M. R.; Jacobson, R. A.; Yang, S.; Ringrose, S. L. *Inorg. Chem.* **1992**, *193*, 143.

(47) van Dijk, M.; Morita, Y.; Petrovic, S.; Sanders, G. M.; van der Plas, H. C.; Stam, C. H.; Wang, Y. *J. Heterocycl. Chem.* **1992**, *29*, 81.

(48) Benson, D. R.; Valentekovich, R.; Knobler, C. B.; Diederich, F. *Tetrahedron* **1991**, *47*, 2401.

Table 4. Selected Structural Parameters for Porphyrins **H$_2$14, H$_2$15, H$_2$16, Ni17, Ni18**, and **Ni19**

	H$_2$14	**H$_2$15**	**H$_2$16**	**Ni17**	**Ni18**	**Ni19**
			Displacements, Å			
24 core atoms[a]	0.10	0.11	0.11	0.36	0.53	0.37
N_4 plane[a]	0.07	0.03	0.01	0	0.12	0.05
Ni[b]				0.02 (0.04)	0.02 (0.08)	0.02 (0.04)
C_m[b]	0.06 (0.06)	0.04 (0.03)	0.14 (0.13)	0.73 (0.73)	0.44 (0.44)	0.68 (0.68)
C_a[b]	0.09 (0.08)	0.08 (0.08)	0.12 (0.08)	0.41 (0.41)	0.37 (0.38)	0.38 (0.38)
C_b[b]	0.20 (0.15)	0.21 (0.21)	0.28 (0.15)	0.28 (0.28)	0.91 (0.91)	0.36 (0.35)
C(5)[b]	0.04 (0.11)[c]	0.05 (0.04)[c]	0.17 (0.10)[c]	0.73 (0.68)[c]	0.45 (0.46)[c]	0.87 (0.90)[c]
C(10)[b]	0.04 (0.02)	0.05 (0.04)	0.02 (0.23)	0.88 (0.96)[c]	0.48 (0.52)[c]	0.62 (0.58)[c]
C(15)[b]	0.13 (0.03)[c]	0.06 (0.05)[c]	0.14 (0.13)[c]	0.66 (0.68)	0.51 (0.37)[c]	0.58 (0.60)[c]
C(20)[b]	0.04 (0.07)	0.01 (0)	0.22 (0.06)	0.64 (0.59)	0.31 (0.40)	0.63 (0.63)
			Bond Lengths and Distances, Å			
core size	2.094	2.096	2.083	1.907	1.909	1.916
N(21)−N(22)	2.695[c]	2.671[c]	2.733[c]	2.687[c]	2.708[c]	2.721[c]
N(22)−N(23)	3.201	3.239	3.143	2.690[c]	2.700[c]	2.686[c]
N(23)−N(24)	2.701[c]	2.659[c]	2.750[c]	2.693	2.694[c]	2.755[c]
N(24)−N(21)	3.214	3.235	3.128	2.718	2.725	2.677
Ni−N(21)				1.909(3)	1.903(4)	1.912(3)
Ni−N(22)				1.902(4)	1.916(4)	1.916(2)
Ni−N(23)				1.913(3)	1.902(4)	1.917(3)
Ni−N(24)				1.904(4)	1.914(4)	1.917(2)
			Bond Angles, deg			
C(4)−C(5)−C(6)	124.4(4)[c]	123.1(3)[c]	125.2(4)[c]	122.4(4)[c]	121.9(4)[c]	120.3(3)[c]
C(9)−C(10)−C(11)	131.8(4)	133.9(3)	131.4(5)	120.1(4)[c]	121.3(4)[c]	122.0(3)[c]
C(14)−C(15)−C(16)	123.5(4)[c]	122.6(3)[c]	123.5(4)[c]	122.9(4)	121.8(4)[c]	124.2(4)[c]
C(19)−C(20)−C(1)	133.3(4)	132.8(3)	131.5(5)	123.8(4)	122.9(5)	122.0(2)

[a] Mean deviation of all atoms in least-squares plane. [b] Deviations from N_4 plane; numbers in parentheses are deviations from the least-squares plane of the 24 core atoms. [c] Meso-R-substituted.

Table 5. Differences in Bond Angles (deg) and N···N Separations (Å) between the Substituted and Unsubstituted Meso Quadrants of Porphyrins **9**−**11** and **13**

	H$_2$9	**H$_2$11**	**H$_2$13**	av	**Ni9**	**Ni10**[a]	**Ni11**	av[a]	%[b]
$C_a-C_m-C_a$	−11.0	−7.9	−8.8	−9.2	−2.9	−4.2	−2.7	−3.5	38
C_m-C_a-N	−7.1	−4.4	−5.4	−5.6	−1.5	−0.7	−1.5	−1.1	20
$C_m-C_a-C_b$	+7.6	+4.3	+5.7	+5.9	+2.6	+2.1	+3.0	+2.0	34
N···N	−0.66	−0.43	−0.52	−0.50	−0.09	−0.09	−0.13	−0.10	20
N−M−N	−23.6[c]	−17.8[c]	−20.0[c]	−20.5[c]	−3.6	−3.5	−5.3	−4.0	20
$C_a-C_b-CH_x$	+8.9	+4.4	+5.4	+6.2	+4.4	+4.4	+6.0	+4.8	77
$C_b-C_b-CH_x$	−6.7	−3.2	−4.6	−4.8	−4.1	−4.1	−5.5	−4.5	94

[a] Includes two independent molecules of **Ni10**. [b] Average difference in the nickel(II) complexes expressed as a percentage of the average difference in the metal-free porphyrins. [c] Calculated from the N···N separation, assuming a hypothetical metal ion centered in the porphyrin core.

are consistent for all three metal-free porphyrins but decrease in size in the order **H$_2$9** > **H$_2$13** > **H$_2$11**. The average changes in bond angle for $C_m-C_a-C_b$, C_m-C_a-N, $C_b-C_b-C_x$, and $C_a-C_b-C_x$ are similar (5.5 ± 0.7°) whereas the change for $C_a-C_m-C_a$ is somewhat larger (9.2°).

The differences in the bond angles are generally much smaller for the nickel complexes, suggesting that metal complexation restricts the ability of the porphyrin to undergo asymmetric in-plane distortions. For example, the differences for the C_m-C_a-N, $C_m-C_a-C_b$, and $C_a-C_m-C_a$ angles and the differences between the two N−N distances and the N−M−N angle (for the metal-free porphyrins the N−M−N angle was calculated from the N−N separations by assuming a hypothetical metal ion centered in the porphyrin core) decrease to 20−38% of their values in the metal-free porphyrins. The differences between the $C_b-C_b-C_x$ and $C_a-C_b-C_x$ angles decrease to a much smaller extent, which is reasonable given that this method of relieving steric strain will be less dependent on whether the porphyrin is complexed to a metal ion.

Finally, a packing analysis was performed for all of the structures. A typical example of the molecular packing for the 5,15-diarylporphyrins is shown for **H$_2$11** in Figure 6. With the exception of **H$_2$13**, which crystallized by formation of parallel running layers of molecules, the 5,15-diaryl compounds crystallized in the general fashion shown in Figure 6. No unusual short intermolecular contacts were found for the two metal-free structures, and no evidence for strong π-overlap and aggregation was seen in the Ni(II) structures. Some overlap of the π-systems was found in **Ni11**, where the separation of the N_4 planes was 3.88 Å. However, the large Ni−Ni separation of 5.96 Å leads to a very weak aggregate structure.[5] Due to the orthogonal arrangement of neighboring molecules in the nickel(II) porphyrin structures, a side-chain hydrogen−nickel contact on the order of 2.7−3.1 Å was observed, although no unusually short intermolecular contacts between peripheral groups or macrocycle atoms were found. In the unit cell of the 5,15-dialkylporphyrin **Ni10**, the planes of the two crystallographically independent molecules form an angle of 61.5°. The Ni−Ni separation in these pairs is 7.41 Å, while the Ni−Ni distance between different layers is 9.82 Å. The crystal packing analysis thus suggests that the very ruffled structures seen for the nickel(II) 5,15-dialkylporphyrins are due mainly to steric effects and not crystal packing forces.

In addition to the symmetric porphyrins, some related asymmetrically substituted porphyrins were also examined (Table 4). Figure 7 shows the molecular structure of the free-base porphyrin **H$_2$14**, which bears a meso-phenyl and a meso-hydroxyethyl group flanked by ethyl substituents. Studies on the 5,15-diarylporphyins (see **H$_2$11** and **H$_2$13**) and 5,15-diethylporphyrins (e.g. **H$_2$10**)[35] have shown that both types of

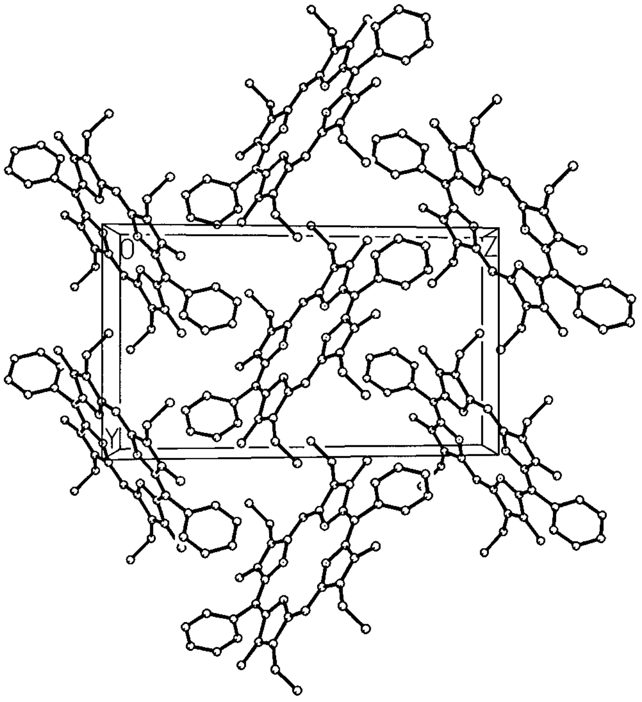

Figure 6. View of the molecular packing in the unit cell of $\mathbf{H_211}$. Hydrogen atoms have been omitted for clarity.

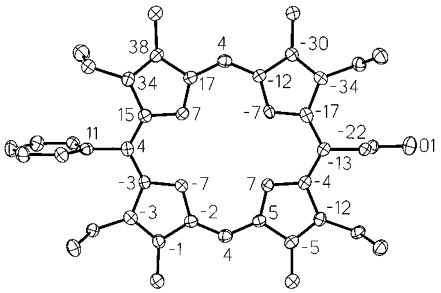

Figure 7. Molecular structure of $\mathbf{H_214}$. Ellipsoids are drawn for 50% occupancy, and hydrogen atoms have been omitted for clarity. Numbers give the deviations of the macrocycle atoms from the least-squares plane of the four nitrogen atoms (Å × 10^2).

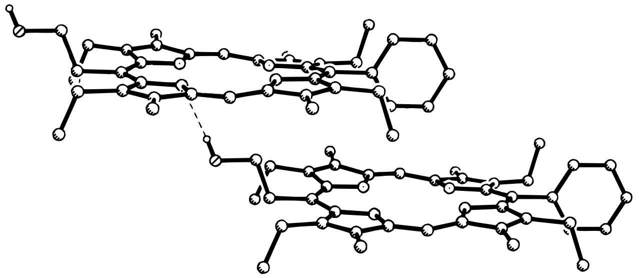

Figure 8. Partial view of the hydrogen-bonded polymer in the crystal of $\mathbf{H_214}$.

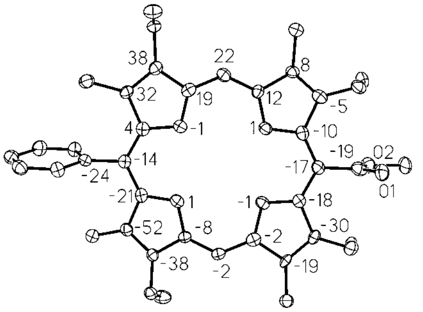

Figure 9. Molecular structure of $\mathbf{H_216}$. Ellipsoids are drawn for 50% occupancy, and hydrogen atoms have been omitted for clarity. Numbers give the deviations of the macrocycle atoms from the least-squares plane of the four nitrogens atoms (Å × 10^2).

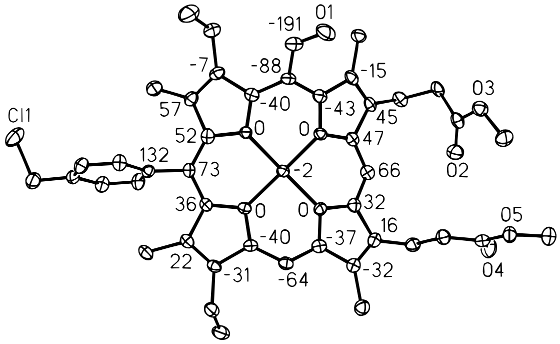

Figure 10. Molecular structure of **Ni17**. Ellipsoids are drawn for 50% occupancy, and hydrogen atoms have been omitted for clarity. Numbers give the deviations of the macrocycle atoms from the least-squares plane of the four nitrogen atoms (Å × 10^2).

porphyrin relieve steric strain mainly by in-plane distortion of the macrocycle. $\mathbf{H_214}$ also shows a rectangular core conformation (N⋯N = 3.21 and 2.70 Å, $\Delta_{N\cdots N} = 0.51$ Å) and significantly different $C_a-C_m-C_a$ angles (132.6° vs 124.0°) (Table 3). The two meso-substituents also show a slight anti orientation with respect to the macrocycle plane similar to that seen for the 5,15-diarylporphyrins.

Some ruffling is observed for one half of the molecule (pyrroles I and II) with C_b displacements on the order of 0.35 Å. This might be the result of packing forces, as $\mathbf{H_214}$ shows a special type of molecular packing in the crystal (Figure 8). Individual molecules are bound together via a hydrogen bond between the hydroxyl group and pyrrole nitrogen [N(24)−O(1) = 3.21 Å; N(24)−H(1A) = 2.38 Å]. This leads to the formation of a hydrogen-bonded polymer in the crystal. The molecules related by hydrogen bonds are not further stabilized by π-interactions. The interplanar separation of neighboring molecules is 4.65 Å, and the centers are separated by 8.09 Å. Individual polymer stacks are separated by solvate molecules of *n*-hexane. However, this arrangement brings the hydroxyethyl group close to pyrrole II of a neighboring molecule; for example atom C(152) is separated from N(22) (a pyrrole nitrogen with strong C_b displacements) by 3.6 Å. On the other hand, the closest contact observed between the phenyl ortho position C(52) and a neighboring pyrrole [N(24)] phenyl is 3.95 Å.

Similar structural results were obtained for $\mathbf{H_215}$ (structure not shown), which has para-chlorophenyl and chloroethyl meso-substituents. $\mathbf{H_215}$ packed in a manner similar to that of $\mathbf{H_214}$, albeit with the shortest intermolecular contact being Cl(1)−H(21) (2.89 Å). $\mathbf{H_216}$ has meso-phenyl and carboxy methyl ester groups (Figure 9). It shows considerable in-plane distortion, as evidenced by inequivalent N⋯N separations (3.14 Å vs 2.74 Å, $\Delta_{N\cdots N} = 0.40$ Å) and $C_a-C_m-C_a$ angles (131.4 vs 124.4°) (Table 3). However, in this case, a nonplanar conformation is observed with modest out-of-plane displacements at both the meso and pyrrole positions. A packing diagram showed that $\mathbf{H_216}$ formed antiparrallel running layer of molecules; the closest intermolecular contacts are between nitrogen atoms and phenyl hydrogen atoms [N(22)−H15(D) = 2.597 Å; N(23)−H(15E) = 2.620 Å].

Ni17 is an example of a porphyrin with a 5,10- rather than 5,15-substitution pattern (Figure 10). The meso-aryl and meso-formyl substituents give rise to a mainly ruffled conformation with some wave distortion and a small amount of doming (Table 3). The displacements of the meso-carbon atoms were larger

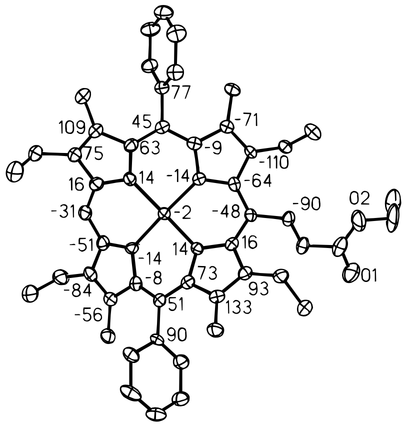

Figure 11. Molecular structure of **Ni18**. Ellipsoids are drawn for 50% occupancy, and hydrogen atoms have been omitted for clarity. Numbers give the deviations of the macrocycle atoms from the least-squares plane of the four nitrogen atoms (Å × 10^2).

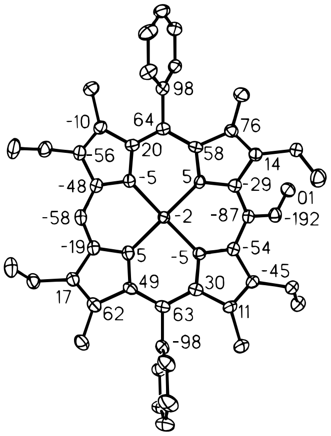

Figure 12. Molecular structure of **Ni19**. Ellipsoids are drawn for 50% occupancy, and hydrogen atoms have been omitted for clarity. Numbers give the deviations of the macrocycle atoms from the least-squares plane of the four nitrogen atoms (Å × 10^2).

than those seen in NiOEP (0.5 Å),[44a] consistent with additional peripheral steric strain arising from the presence of the meso-substituents. The overall degree of nonplanarity was similar to that found in the 5,15-dialkyl-substituted porphyrins **Ni9** and **Ni10**. In line with the asymmetric substitution pattern, the distortion mode is asymmetric and there are smaller deviations from planarity for pyrroles III and IV and larger displacements of the substituted C_m positions compared to the unsubstituted ones.[49]

The structures of two undecasubstituted Ni(II) porphyrins, **Ni18** and **Ni19**, are shown in Figures 11 and 12, respectively. The crystal structure of **Ni18** (Figure 11) shows a mixture of ruffle and saddle distortions with minor contributions from other distortion modes. The large displacements of the C_m positions (average 0.44 Å) and the out-of-plane displacements of individual C_b positions [e.g., 1.33 Å for C(18)] indicate that the molecule is very distorted. The largest C_6 displacement is comparable with those seen in highly nonplanar dodecasubstituted porphyrins.[15] The distortion mode is also asymmetric, although the differences between sterically “overloaded” parts of the molecule and those without meso-substituents are less pronounced than those seen in the decasubstituted porphyrins. Interestingly, the only difference between **Ni19** (Figure 12) and **Ni18** is the exchange of a meso-formyl for a meso-acrylate group, yet the total nonplanar distortion decreases markedly and the contributions of ruffled and saddle distortion modes are reversed (Table 3).

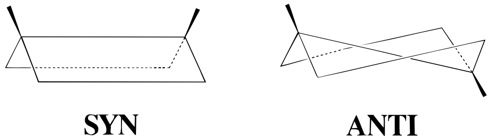

Figure 13. Solution structures previously proposed for $\mathbf{H_29}$ and **Zn9**.[29] Wedges indicate the substituents at the 5- and 15-positions.

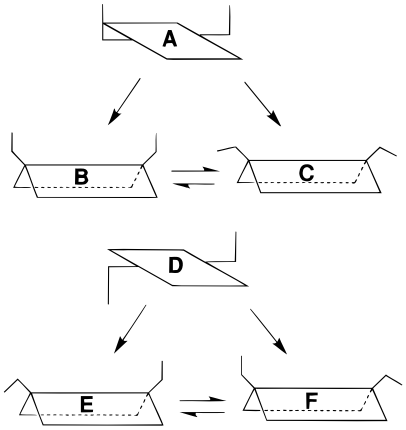

Figure 14. Representations of the structures and the conformational equilibria proposed for decaalkylporphyrins in solution (see text for discussion).[35]

As might be expected, an analysis of the molecular packing of the asymmetrically substituted Ni(II) porphyrins gave no evidence that the observed nonplanarity was due to packing forces. In most cases, the individual molecules showed intermolecular contacts of the non-hydrogen atoms of >4 Å. **Ni17** shows some degree of overlap of the π-systems in the crystal. These weak dimers are characterized by an interplanar separation of 3.89 Å, a Ni−Ni separation of 5.77 Å, and a lateral shift of the metal centers of 4.28 Å. The shortest intermolecular contact found was H(13A)−N(23) at 2.615 Å. **Ni19** shows a molecular packing similar to that found for many other nonplanar saddle-shaped porphyrins with the molecules arranged in a such a way that the concave shapes face and interlock with each other. The closest contact observed is 2.519 Å between O(1) and H(18A). **Ni18** adopts a similar structure with the closest contact being Ni−H(15D) (3.136 Å).

Proton NMR Spectroscopy. Proton NMR spectra of the free-base and zinc(II) complexes of **9** and other related decaalkylporphyrins are temperature dependent and show two species at low temperatures.[29,35] These species were initially assigned to syn and anti conformations of the porphyrin macrocycle as shown in Figure 13,[29] although subsequent studies suggested that cis and trans conformations of the meso-substituents due to hindered rotation about the $C_m-C_{substituent}$ bond was a more likely explanation for the observed NMR properties of $\mathbf{H_29}$, **Zn9**, and **Ni9**.[35] The main points of the cis/trans model proposed for 5,15-substituted porphyrins[35] can be summarized as follows: (1) The conformation of the porphyrin macrocycle can be planar (A and D) or roof-shaped (B, C, E, and F) with cis (A−C) or trans (D−F) ethyl orientations (Figure 14). (2) The energy difference between the planar conformations A and D is small, but as the porphyrin becomes nonplanar, axial ethyl groups (B) are favored over equatorial groups (C). (3) There is an energy increase in the series B < E = F < C which becomes more marked as the porphyrin becomes more nonplanar. (4) Conformations B and C or E and F are in equilibrium due to inversion of the porphyrin macrocycle.

---

(49) Kalisch, W. W.; Senge, M. O. *Tetrahedron Lett.* **1996**, *37*, 1183.

Table 6. Proton NMR Data

	$\mathbf{H_211}$	$\mathbf{H_210}$		$\mathbf{H_29}$		**Zn10**		**Zn9**		**Ni11**	**Ni10**	**Ni9**	$\mathbf{H_410^{2+}}$		$\mathbf{H_49^{2+}}$	
	293 K	296 K	223 K	293 K	233 K	293 K	233 K	293 K	233 K	293 K	273 K	293 K	293 K	183 K	298 K	183 K
meso-H	10.19	10.05	10.06	10.08	10.13 10.10	9.90	9.85 9.88	9.91	9.99 9.88	9.45	9.06	9.07	9.96	10.05(1) 10.02(2) 9.97(1)	10.00	10.11(1) 10.05(2) 9.97(1)
H_o/CH_2	8.06	5.12	5.10 5.09	5.02	4.97	5.18	5.13	5.06	5.00	7.83	4.40	4.36	4.87	4.83	4.81	4.72
H_m/CH_3	7.76	1.95	1.96 1.94	1.79	1.92 1.81	1.69	1.82	1.30 1.64	1.26	7.63 1.73	0.67	0.67	2.08	1.99	2.08	1.99
H_p	7.82									7.69						
CH_3	2.50	3.65	3.64	3.61	3.61 3.60	3.66	3.63 3.62	3.54	3.51 3.56	2.23	3.34	3.20	3.21	3.21 3.15	3.18	3.15
CH_2CH_3 (C*H*₂)	4.03	4.13	4.15 4.10	4.02	4.04 3.92	4.07	4.04	4.03	4.00	3.69	3.67	3.74	3.72	3.72	3.58	3.78 3.57 3.37
CH_2CH_3 (C*H*₃)	1.81	1.89	1.86	1.79	1.77 1.75	1.85	1.81	1.83	1.82	1.59	1.58	1.72	1.34	1.18	1.44	1.99 1.01
NH	−2.51	−1.91	−2.19	−1.78	−1.98								−2.10	−2.85	−2.78	−2.89
K		1		1.14		1.20		2.8					∼1		∼1	
Δ*G*		0.0 (233 K)		0.1 (233 K)		0.1 (233 K)		0.5 (243 K)								
Δ*G** (ethyl rotation)		14.5 (273 K)		14.3 (273 K)		13.5 (263 K)		13.6 (273 K)					9.8 (198 K)		9.9 (203 K) 12.3 (253 K)	

We first compared the previously published NMR data for $\mathbf{H_29}$, **Zn9**, and **Ni9**[35] with those of the structural isomer **10** where the meso-ethyls are flanked by methyl groups rather than ethyl groups. All of the signals expected for the two species could not be resolved at low temperature for the free-base porphyrins. However, the chemical shifts and thermodynamic and kinetic data for the free-base or nickel(II) complexes were found to be essentially independent of the flanking substituents (Table 6). This suggests that the arrangement of the pyrrole substituents has little effect on the solution structure, a result consistent with the similar crystal structures seen for **Ni9**[35] and **Ni10** (Figure 4). The solution structure of $\mathbf{H_210}$ might best be described[35] in terms of a mixture of conformations A and D, and the structure of **Ni10**, in terms of conformation B, which is the lowest energy nonplanar structure. However, for **Zn9** and **Zn10** the ratio of the two species and the chemical shifts of the meso-methyl groups are different, suggesting that the groups flanking the meso-ethyl groups perturb the conformation of the porphyrin macrocycle. In this case, the smaller equilibrium constant seen for **Zn10** (1.20 vs 2.8 for **Zn9**) and the smaller chemical shift difference between the cis and trans species (0.18 ppm for **Zn10** vs 0.47 ppm for **Zn9**) both suggest a slightly more planar conformation when the flanking substituents are methyl groups.

Porphyrins **10** and **11** were then compared to determine the effect of changing the meso-substituents from ethyl groups to phenyl groups. No dynamic processes were observed when $\mathbf{H_211}$ and **Ni11** were cooled to 193 K. Furthermore, the ortho or meta protons of the phenyl rings appeared as single signals, contrary to what one might expect on the basis of the anti arrangement of the phenyl rings seen in the crystal structures of $\mathbf{H_211}$ (Figure 1) and **Ni11** (Figure 3). There are likely several factors underlying the behavior of $\mathbf{H_211}$ and **Ni11**. Obviously, rotational isomerism of the kind seen for the 5,15-diethylporphyrins is not possible for the 5,15-diphenylporphyrins because of the symmetry of the phenyl groups. The planar crystal structure of $\mathbf{H_211}$ (Figure 1) and the shallow saddle conformation seen for **Ni11** (Figure 3) also suggest a minimal barrier for nonplanar conformational distortions in the 5,15-diphenylporphyrins. It is therefore likely that the chemical shifts of the ortho or meta protons are averaged by molecular motions of the porphyrin.

Because the dications of 5,15-disubstituted porphyrins were not previously investigated, we also studied the dications of porphyrins **9** and **10** ($\mathbf{H_49^{2+}}$ and $\mathbf{H_410^{2+}}$) by variable-temperature proton NMR spectroscopy. The proton spectrum of $\mathbf{H_49^{2+}}$ showed additional signals for the meso, NH, and pyrrole CH_3 protons at low-temperatures ($\Delta G^* = 9.8$ kcal mol^{-1}), with the meso protons splitting into three signals of ratio 1:2:1 (Table 6). For $\mathbf{H_410^{2+}}$, the pyrrole methylene protons initially became diastereotopic ($\Delta G^* = 12.3$ kcal mol^{-1}), followed by a second dynamic process which again caused splitting of the meso protons (1:2:1 pattern), the NH protons, and the pyrrole CH_2 and CH_3 protons ($\Delta G^* = 9.8$ kcal mol^{-1}). The unusual 1:2:1 pattern for the meso protons H(10) and H(20) in $\mathbf{H_49^{2+}}$ and $\mathbf{H^410^{2+}}$ can be explained by hindered rotation of the meso-ethyl groups ($\Delta G^* = 9.8$ kcal mol^{-1}) and a *saddle* conformation of the porphyrin macrocycle (a saddle conformation is not unreasonable because it will minimize repulsions between the four core hydrogens of the dication). In the saddle structures seen for the free base,[15g] the dications[15h] and metal complexes[15a−c] of **3**, the 5,15-meso-phenyl groups are twisted with respect to the porphyrin plane (Figure 15A). By analogy, saddle structures for $\mathbf{H_49^{2+}}$ and $\mathbf{H_410^{2+}}$ with ethyl rotation slow on the NMR time scale could give cis or trans meso-ethyl orientations (Figure 15B,C). One meso proton signal would be seen for the cis orientation and two signals for the trans orientation, thereby producing the observed 1:2:1 pattern if the cis and trans conformations were about equally populated. Note that a process with a similar barrier ($\Delta G^* = 9.3$ kcal mol^{-1}) was seen for $\mathbf{H_45b^{2+}}$ and was also assigned to hindered rotation of the meso-ethyl groups.[16b] Also, the barriers for rotation of the ethyl groups in the dications are significantly lower than those seen for the free-base porphyrins (8.8−8.9 vs 14.3−14.5 kcal mol^{-1}). The second dynamic process for $\mathbf{H_410^{2+}}$ ($\Delta G^* = 12.3$ kcal

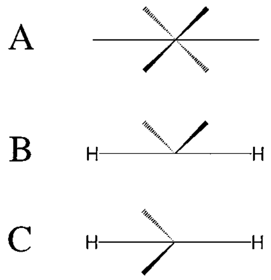

Figure 15. Representations of saddle conformations: (A) the free-base porphyrin[15g] and metal complexes[15a−c] of **3**; (B) *cis*-$\mathbf{H_49^{2+}}$ or -$\mathbf{H_410^{2+}}$; (C) *trans*-$\mathbf{H_49^{2+}}$ or -$\mathbf{H_410^{2+}}$ (see text for discussion).

Table 7. Absorption Maxima (nm) for Free-Base and Nickel Porphyrins in CH_2Cl_2

no.	free-base $Q_x(0,0)$	Ni(II) complex $Q(0,0)$
	“Planar” Reference Compounds	
1	618	551[18b]
2	646[18c]	557[18b]
	“Nonplanar” Reference Compounds	
3	706[18c]	585[18b]
4	724[16b]	613[16b]
	Decasubstituted 5,15-Compounds	
9	632[35]	578, 596[35]
10	648	580
11	624	562
12	623[33b]	562
13	624	564

mol^{-1}) may be macrocyclic inversion as $\Delta G_{\text{inversion}}^* = 11.8$ kcal mol^{-1} in **H$_4$5b^{2+}**.

The examples reported in this and our earlier study of 5,15-substituted porphyrins[35] require revised explanations of the NMR data for the nickel(II) complexes of porphyrins **5a**−**c**[16b] and the free bases and zinc(II) complexes of other 5,15-substituted decalkylporphyrins.[29] Previously, a dynamic process observed for **Ni5b** ($\Delta G^* = 11.2$ kcal mol^{-1}) and **Ni5c** ($\Delta G^* = 12.5$ kcal mol^{-1}) but not for **Ni5a** ($\Delta G^* < 8.0$ kcal mol^{-1}) was assigned to macrocyclic inversion. Another macrocyclic inversion process which occurred with retention of the relative orientations of the ethyl groups was also invoked, and required to be fast on the NMR time scale at all of the temperatures studied in order to explain the NMR data. From the present study, it is clear that the dynamic process observed for **Ni5b** and **Ni5c** was not macrocyclic inversion but hindered rotation of the meso-alkyl groups and that the lower energy process that was fast on the NMR time scale was indeed inversion of the macrocycle with retention of the relative orientations of the ethyl groups. This revised model explains why there was no observable dynamic process for **Ni5a** where R^2 is a symmetrical methyl group. A similar argument can also be used to rationalize the absence of two species at low temperatures for **9** where $R^4 = CH_3$.[29]

Optical and Resonance Raman Spectroscopy. Recent studies demonstrated significant differences between the optical spectra[2,15,16,18,19] and excited state properties[15e] of nonplanar dodecasusbstituted porphyrins such as OETPP (**3**) and DPP (**4**) and those of regular porphyrins such as OEP (**1**) and TPP (**2**). The principal difference in the optical spectra is a shift to longer wavelengths for the absorption maximum of the first electronic excited state [$Q_x(0,0)$ for free-base porphyrins or $Q(0,0)$ for metal complexes], which can be used as an indicator of the degree of macrocycle nonplanarity. Theoretical calculations indicate that the underlying mechanism of the observed red shift is a destabilization of the porphyrin HOMO and a significantly smaller perturbation of the LUMO.[2,15b,c]

The absorption maxima [$Q_x(0,0)$] for the free bases of porphyrins **9**−**13** were compared with those of the less subsituted and essentially planar reference compounds **H$_2$1** and **H$_2$2** and the very nonplanar dodecasubstituted reference compounds **H$_2$3** and **H$_2$4** (Table 7). The [$Q_x(0,0)$] bands for **H$_2$1** and **H$_2$2** are seen at 618 and 646 nm, whereas for **H$_2$3** and **H$_2$4** the absorption maxima exhibit large bathochromic shifts ($\lambda_{\max} = 706$ and 724 nm for **H$_2$3** and **H$_2$4**, respectively). The absorption maxima for the free bases of porphyrins **9**−**13** encompass a range similar to that seen for the essentially planar reference compounds **H$_2$1** and **H$_2$2**, suggesting that all of the free-base 5,15-diaryl- and 5,15-diethylporphyrins adopt planar or nearly planar conformations in solution. The results obtained from the optical studies are therefore consistent with the available crystallographic data, which show essentially planar conformations with elongation of the porphyrin core along the 5,15-axis [e.g. **H$_2$11** (Figure 1), **H$_2$13** (Figure 2), and **H$_2$9**[35]].

Table 8. Resonance Raman Data (cm^{-1}) for Nickel(II) Porphyrins

	ν_2	ν_3	ν_4	ν_{10}
Ni1, planar triclinic B (crystal)[18b]		1525	1383	1662
Ni3 (crystal)[18b]	1566	1507	1360	
Ni3 (CS_2)[15b]	1562	1505	1360	
Ni10 (CS_2)	1580	1500	1357	1614
Ni11 (CS_2)	1589	1515	1361	1631

Absorption maxima for the nickel(II) complexes of porphyrins **9**−**11** are also summarized in Table 7. The [$Q(0,0)$] bands for the less subsituted and planar or slightly nonplanar reference compounds **Ni1** and **Ni2** are found at similar wavelengths (551 and 557 nm). Absorption maxima for the very nonplanar dodecasubstituted reference compounds **Ni3** and **Ni4** are red-shifted by 30−60 nm ($\lambda_{\max}$, nm (ϵ, M^{-1} cm^{-1}): 585 and 613 nm, respectively). The nickel complexes of the 5,15-diphenyl-substituted porphyrins have absorption maxima similar to those of the regular porphyrins (562−564 nm), indicating planar or nearly planar structures in solution. This is consistent with crystallographic data for the 5,15-diphenyl-substituted porphyrins, which show planar or only slightly nonplanar structures [e.g., **Ni11** shows a shallow saddle structure (Figure 3) and **Ni12** a planar structure (structure not shown)]. The nickel complexes of the 5,15-ethyl-substituted porphyrins show a shift to absorption at longer wavelength, with $\lambda_{\max}$ being approximately 580 nm (an additional band at 596 nm was seen for **Ni9**). This bathochromic shift suggests a more nonplanar conformation than was seen for the 5,15-diphenylporphyrins, which again agrees with the very nonplanar crystal structures seen for **Ni10** (Figure 3) and **Ni9**.[35] Overall, the optical studies agree with the results obtained from crystallographic investigations. This reinforces the idea that optical spectrospcopy is a useful tool for investigating porphyrin nonplanarity in solution, provided there are reasonably large nonplanar deformations but only small electronic perturbations from the substituents.

Resonance Raman spectroscopy provides another technique for determining if porphyrins adopt nonplanar conformations in solution, with significant differences being observed between the resonance Raman spectra of metal complexes of nonplanar dodecasusbstituted porphyrins such as **3** and **4** and metal complexes of regular porphyrins such as **1** and **2**.[15b,d,18a−c,20e,50] For example, increased nonplanarity has been shown to correlate with a shift to lower frequency for structure-sensitive lines (e.g. ν_2, ν_3, and ν_4) in a series of nickel(II) porphyrins.[18a−c] Table 8 summarizes the frequencies of several structure-sensitive Raman lines for **Ni1**, **Ni3**, **Ni10**, and **Ni11.** The frequencies of the structure-sensitive lines for **Ni10** and **Ni11** typically fall midway between those of the regular porphyrin **Ni1** and the very nonplanar dodecasubstituted porphyrin **Ni3**. Lower frequencies are also seen for **Ni10** compared to **Ni11**, suggesting a more nonplanar conformation for **Ni10**. This is again consistent with the crystallographic data discussed previously. Interestingly, extensive broadening of the ν_{10} line is seen for **Ni11** but not for **Ni10**. The mostly likely explanation for this broadening is the presence of multiple porphyrin conformations in solution, a phenomenon which has been observed for NiOEP.[44c] This result agrees with crystallographic data for **Ni11** and **Ni12**

---

(50) (a) Shelnutt, J. A.; Majumder, S. A.; Sparks, L. D.; Hobbs, J. D.; Medforth, C. J.; Senge, M. O.; Smith, K. M.; Miura, M.; Luo, L.; Quirke, J. M. E. *J. Raman Spectrosc.* **1992**, *23*, 523. (b) Sparks, L. D.; Anderson, K. K.; Medforth, C. J.; Smith, K. M.; Shelnutt, J. A. *Inorg. Chem.* **1994**, *33*, 2297.

showing that the 5,15-diaryl-substituted porphyrins can exist in both planar and nonplanar conformations.

Conclusions

A comparative analysis of the conformations of eight 2,3,5,7,8,12,13,15,17,18-decasubstituted porphyrins determined by X-ray crystallography reveals that peripheral steric strain in these systems can be relieved via in-plane and/or out-of-plane distortions. This is in contrast to the case of dodecasubstituted porphyrins, which minimize steric strain principally by out-of-plane distortions,[15,16,19b,20c] or to the case of mono-meso-substituted octaalkylporphyrins bearing small substituents, where similar conformational analyses can sometimes be ambiguous because steric effects can be masked by the influence of packing forces.[31b]

Free-base porphyrins with 5,15-diaryl, 5,15-dialkyl, or mixtures of alkyl and aryl substituents at the 5- and 15-positions show small or negligible out-of-plane distortions but significant in-plane distortions. The in-plane distortions give rise to a specific pattern of bond angle changes, and to an unusual elongation of the porphyrin core along the 5,15-axis which makes the macrocycle appear oblong rather than square. A review of the literature reveals that this in-plane distortion is conserved for other 5,15-substituted free-base porphyrins and is also present to a lesser degree in free-base octalkylporphyrins with only one meso-substituent. Nickel(II) complexes of the 5,15-dialkyl-substituted porphyrins adopt highly ruffled conformations, suggesting that steric repulsions are relieved by nonplanar distortions of the macrocycle. However, there is also a small amount of in-plane distortion along the 5,15-axis which is qualitatively similar to that seen for the free-base porphyrins. Crystal structures of other metal complexes of 5,15-dialkyl-substituted porphyrins also show ruffled conformations, suggesting that this is an intrinsic feature of this class of porphyrins. Nickel(II) complexes of 5,15-diaryl-substituted porphyrins show both planar and saddle conformations. Again, there is a small but significant elongation along the 5,15-axis which is qualitatively similar to that seen for the free-base 5,15-substituted porphyrins. Published structures of other nickel(II) 5,15-diaryl-substituted porphyrins show ruffled conformations. Taken as a whole, these results suggest that this group of porphyrins is conformationally flexible and not intrinsically nonplanar.

Crystal structures of the nickel(II) complexes of a 5,10-disubstituted porphyrin and two 5,10,15-trisubstituted porphyrins reveal macrocycles that are very distorted and exhibit varying degrees of nonplanarity characterized mainly by ruffle and saddle distortions, implying that these macrocycles are permanently distorted. Interestingly, a fairly minor structural change for the 5,10,15-substituted porphyrins (exchanging a meso-formyl for a meso-acrylate group) markedly decreases the degree of nonplanarity and reverses the contributions of ruffle and saddle distortion modes. This suggests that the 5,10,15-trisubstituted porphyrins are most likely conformationally flexible. On this point, it is interesting to note that marked conformational flexibility was recently demonstrated for dodecasubstituted porphyrins using a series of dodecaphenylporphyrins.[51]

A spectroscopic analysis of the 5,15-dialkyl- and 5,15-diarylporphyrins using optical, resonance Raman, and ^{1}H NMR techniques suggested that the structural trends seen in the crytsalline state were retained in solution. For example, absorption maxima for the metal-free 5,15-dialkyl- and 5,15-diaryl-substituted porphyrins and the nickel(II) complexes of the 5,15-diarylporphyrins were comparable to those of regular porphyrins, whereas those for nickel(II) complexes of the 5,15-diarylporphyrins showed a shift to longer wavelength, indicating nonplanar conformations. Variable-temperature ^{1}H NMR experiments confirmed our earlier suggestion[35] that the dynamic process seen for the 5,15-dialkylporphyrins is hindered rotation of the meso-substituents and not interconversion between two different nonplanar porphyrin structures.[29]

Acknowledgment. This work was supported by grants from the National Science Foundation (K.M.S., CHE-96-23117), the Fonds der chemischen Industrie and the Deutsche Forschungsgemeinschaft (M.O.S., Se543/2-1 and 2-2 and Sfb377), and the U.S. Department of Energy (J.A.S., DE-ACO4-94AL85000).

Supporting Information Available: Listings of complete bond lengths, bond angles, anisotropic thermal parameters, and atomic coordinates and isotropic thermal parameters, along with figures showing atom numbering for all crystal structures, thermal ellipsoid plots for **Ni12** and **H$_2$15**, packing plots for **Ni11**, **H$_2$13**, **Ni10**, **H$_2$14**, **Ni17**, and **Ni19**, a side view of the molecular structure of **H$_2$13**, and deviations from the four-nitrogen least-squares plane for **Ni12** and **H$_2$15** (112 pages). Ordering information is given on any current masthead page.

IC961156W

---

(51) Nurco, D. J.; Medforth, C. J.; Forsyth, T. P.; Olmstead, M. M.; Smith, K. M. *J. Am. Chem. Soc.* **1996**, *118*, 10918.